NATIONAL ADVISORY COMMITTEE FOR AERONAUTICS

TECHNICAL NOTE

TN No. 1049

ANALYSIS OF AVAILABLE DATA ON THE EFFECTS OF TABS ON CONTROL-SURFACE HINGE MOMENTS

By Stewart M. Crandall and Harry E. Murray

Langley Memorial Aeronautical Laboratory
Langley Field, Va.

Washington
May 1946

E R R A T A

NACA TN No. 1049

ANALYSIS OF AVAILABLE DATA ON THE EFFECTS OF TABS ON CONTROL-SURFACE HINGE MOMENTS

By Stewart M. Crandall and Harry E. Murray

May 1946

On page 2, line 21, reference 21 should be changed to reference 20.

The numbers of references 12 to 21 in tables I and III should be reduced by one.

NATIONAL ADVISORY COMMITTEE FOR AERONAUTICS

TECHNICAL NOTE NO. 1049

ANALYSIS OF AVAILABLE DATA ON THE EFFECTS OF TABS ON CONTROL-SURFACE HINGE MOMENTS

By Stewart M. Crandall and Harry E. Murray

SUMMARY

An analysis was made of the hinge-moment effectiveness of tabs based on the available two- and three-dimensional tab data. The results of the analysis indicated that the effects of tabs on control-surface hinge moments can be estimated from geometric characteristics of the tab-flap-airfoil combination with a reasonable degree of accuracy.

In general the tab effect on the control-surface hinge moments is reduced by increasing the airfoil trailing-edge angle and by any alteration of the airfoil surface condition or of the air stream, such as moving the transition forward, roughening the surface, or increasing the turbulence, that tends to increase the boundary-layer thickness near the trailing edge. The tab hinge-moment effectiveness may either increase or decrease with Reynolds number. Whether an increase or a decrease occurs depends on the range of Reynolds number under consideration and on the surface condition of the airfoil.

Gaps at flap and tab hinges reduced the effect of tabs on flap hinge moments, the reduction resulting from tab gaps generally being so large as to make seals advisable. No consistent variation with angle of attack was found for the effect of tabs on hinge moments. A tab, however, may retain a reasonable part of its hinge-moment effectiveness through and beyond the stall. Flap deflection decreases the hinge-moment effectiveness of balancing tabs and increases that of unbalancing tabs.

The available high-speed data indicated that the tab hinge-moment effectiveness decreases as the Mach number

increases; however, tabs may retain a relatively large part of their effectiveness through the subcritical range of Mach number.

INTRODUCTION

In an effort to provide satisfactory methods for predicting control-surface characteristics, the NACA has undertaken a program of summarizing, analyzing, and correlating the results of various experimental investigations of airplane control surfaces. A collection of balanced-aileron test data is given in reference 1. Reference 2 presents a collection of data applicable to the design of tail surfaces. The results of analyses of data for control surfaces with internal balances, plain-overhang and Frise balances, beveled trailing edges, and unshielded horn balances have already been published in references 3 to 6. An analysis of the lift effectiveness of control surfaces is presented in reference 7. The present report gives the results of an analysis of the tab hinge-moment effectiveness based on the tab data of references 1 and 2 with additional data from references 8 to 2D. The terms flap and control surface are used synonymously in the present report. The data were obtained for the most part under conditions of low Reynolds number, high turbulence, and low Mach number.

No data are presented on the tab lift effectiveness, which determines the loss in control-surface lift effectiveness resulting from balancing-tab action, because this control-surface-lift effect can be evaluated as indicated by the analysis of reference 7.

COEFFICIENTS AND SYMBOLS

c_{h_f} flap section hinge-moment coefficient $\left(\frac{h_f}{q{c_f}^2}\right)$

C_{h_f} flap hinge-moment coefficient $\left(\frac{H_f}{q{\bar{c}_f}^2 b_f}\right)$

C_{h_t} tab hinge-moment coefficient $\left(\frac{H_t}{q{\bar{c}_t}^2 b_t}\right)$

P_R resultant pressure coefficient $\left(\frac{p_L - p_U}{q}\right)$

P_{δ_t} average of values of $\left(\frac{\partial P_R}{\partial \delta_t}\right)$ along part of flap balance across tab span

c_l airfoil section lift coefficient $\left(\frac{l}{qc}\right)$

where

l airfoil section lift

h_f flap section hinge moment

H_f flap hinge moment

H_t tab hinge moment

q dynamic pressure

c average airfoil chord across tab span

δ_t tab deflection with respect to flap, degrees

c_f average flap chord across tab span

$\overline{c}_f$ root-mean-square chord of flap

$\overline{c}_t$ root-mean-square chord of tab

p_U static pressure on upper surface of airfoil

p_L static pressure on lower surface of airfoil

b_t span of tab

b_f span of flap

and

ΔC_{h_f} increment of flap hinge-moment coefficient

q_t dynamic pressure of air stream over tab

c_b	average chord of overhang balance across tab span
$\bar{c}_f'$	root-mean-square chord of part of flap spanned by tab
c_t	average tab chord behind tab hinge line
t_f	average across tab span of flap thickness at flap hinge line
ϕ	average across tab span of airfoil trailing-edge angle
y_1	distance from plane of symmetry to inboard end of flap
y_2	distance from plane of symmetry to outboard end of flap
y_3	distance from inboard end of flap to inboard end of tab
y_4	distance from inboard end of flap to outboard end of tab
δ_f	flap deflection with respect to airfoil chord, degrees
α	airfoil angle of attack
α_i	induced angle of attack
λ	taper ratio $\left(\dfrac{\text{tip chord}}{\text{root chord}}\right)$
A	aspect ratio
β	basic tab hinge-moment effectiveness curve deduced from section data
B	basic tab hinge-moment effectiveness curve deduced from finite-span data
τ	turbulence factor
R	Reynolds number

M	Mach number	
K_c'	preliminary chord factor	$\left(1 + 0.51\left(\frac{c_t}{c_f}\right)^{-0.69}\frac{c_f}{c}\right)$
K_t	area-moment factor	$\left(\frac{b_t\bar{c}_f'^2}{b_f\bar{c}_f^2}\right)$
K_b	balance factor	$\left(1 - 0.85\left[\left(\frac{c_b}{c_f}\right)^2 - \left(\frac{t_f}{2c_f}\right)^2\right]\right)$
K_ϕ	trailing-edge-angle factor	$(1.3 - 0.026\phi)$
K_c	revised chord factor	$\left(\left(\frac{c_t}{c_f}\right)^{0.70} + 0.51\frac{c_f}{c}\right)$
$\frac{\partial\delta_t}{\partial\delta_f}$	rate of change of tab deflection with respect to flap deflection for a linked tab	

Subscripts

f	flap
t	tab
b	balance
ϕ	trailing-edge angle
c	chord

The subscripts to partial derivatives denote the factors held constant when the partial derivative is taken.

DATA AND SCOPE

The data used in the correlation were obtained from pressure-distribution tests on NACA 0009 sections summarized in reference 2 and from force tests on various model configurations, the characteristics of which are given in tables I and II. These data came from the following ranges of tab variables: tab-flap chord ratio from 0.10 to 0.50, flap-airfoil chord ratio from 0.12 to 0.60, and trailing-edge angle from 7° to 31°. Sufficient data were available from which to draw quantitative conclusions concerning the effects of changing the size of the tab relative to the flap-airfoil combination, the effect of trailing-edge angle, and the effect of control-surface overhang balance on the tab hinge-moment effectiveness. Insufficient data were available to determine quantitatively the effect of the parameters that varied the tab hinge-moment effectiveness by changing the boundary-layer thickness over the tab. Sufficient data were available, however, upon which to base qualitative conclusions concerning such effects.

BASIC ASSUMPTIONS

The following relationship gives the rate of change of the total hinge-moment coefficient with control-surface deflection for a control surface having a linked tab:

$$\left(\frac{\partial C_{h_f}}{\partial \delta_f}\right)_{\alpha} = \left(\frac{\partial C_{h_f}}{\partial \delta_f}\right)_{\alpha,\delta_t} + \frac{\partial \delta_t}{\partial \delta_f}\left(\frac{\partial C_{h_f}}{\partial \delta_t}\right)_{\alpha,\delta_f}$$

$$+ \frac{b_t \bar{c}_t^{\,2}}{b_f \bar{c}_f^{\,2}}\left[\frac{\partial \delta_t}{\partial \delta_f}\left(\frac{\partial C_{h_t}}{\partial \delta_f}\right)_{\alpha,\delta_t} + \left(\frac{\partial \delta_t}{\partial \delta_f}\right)^2\left(\frac{\partial C_{h_t}}{\partial \delta_t}\right)_{\alpha,\delta_f}\right]$$

The first term represents the hinge moment of the control surface with tab fixed. The second term represents the change in hinge moment resulting from tab deflection. The third term represents the hinge moment required to deflect a tab that is linked to the control surface. Only the second term was investigated for this report.

The important parameter is $\left(\frac{\partial C_{h_f}}{\partial \delta_t}\right)_{\alpha,\delta_f}$, which will hereinafter be referred to as "the tab-hinge-moment effectiveness." A decrease in tab-hinge-moment effectiveness will correspond to numerical values of $\left(\frac{\partial c_{h_f}}{\partial \delta_t}\right)_{\alpha,\delta_f}$ becoming nearer zero.

Under the assumptions of lifting-line theory the finite-span hinge-moment parameters $\left(\frac{\partial C_{h_f}}{\partial \delta_f}\right)_{\alpha,\delta_t}$ and $\left(\frac{\partial C_{h_f}}{\partial \delta_t}\right)_{\alpha,\delta_f}$ may be estimated from section data by means of the following equations (see reference 21):

$$\left(\frac{\partial C_{h_f}}{\partial \delta_f}\right)_{\alpha,\delta_t} = \frac{1}{\frac{b_f}{b/2}\,\bar{c}_f^{\,2}}\left[\int_{\frac{y_1}{b/2}}^{\frac{y_2}{b/2}}\left(\frac{\partial c_{h_f}}{\partial \delta_f}\right)_{\alpha,\delta_t} c_f^{\,2}\, d\left(\frac{y}{b/2}\right) - \int_{\frac{y_1}{b/2}}^{\frac{y_2}{b/2}}\left(\frac{\partial c_{h_f}}{\partial \alpha}\right)_{\delta_f,\delta_t}\left(\frac{\partial \alpha}{\partial \delta_f}\right)_{c_l,\delta_t}\frac{\alpha_i}{\alpha}\, c_f^{\,2}\, d\left(\frac{y}{b/2}\right)\right]$$

and

$$\left(\frac{\partial C_{h_f}}{\partial \delta_t}\right)_{\alpha,\delta_f} = \frac{1}{\frac{b_f}{b/2}\,\bar{c}_f^{\,2}}\left[\int_{\frac{y_1}{b/2}}^{\frac{y_2}{b/2}}\left(\frac{\partial c_{h_f}}{\partial \delta_t}\right)_{\alpha,\delta_f} c_f^{\,2}\, d\left(\frac{y}{b/2}\right) - \int_{\frac{y_1}{b/2}}^{\frac{y_2}{b/2}}\left(\frac{\partial c_{h_f}}{\partial \alpha}\right)_{\delta_f,\delta_t}\left(\frac{\partial \alpha}{\partial \delta_t}\right)_{c_l,\delta_f}\frac{\alpha_i}{\alpha}\, c_f^{\,2}\, d\left(\frac{y}{b/2}\right)\right]$$

If both flap and tab are constant percentage chord and the tab covers the full span of the flap, it can be shown from the two foregoing equations that

$$\frac{\left(\frac{\partial c_{h_f}}{\partial \delta_t}\right)_{\alpha,\delta_f} - \left(\frac{\partial C_{h_f}}{\partial \delta_t}\right)_{\alpha,\delta_f}}{\left(\frac{\partial c_{h_f}}{\partial \delta_t}\right)_{\alpha,\delta_f}} = \frac{\left(\frac{\partial \alpha}{\partial \delta_t}\right)_{c_l,\delta_f}}{\left(\frac{\partial \alpha}{\partial \delta_f}\right)_{c_l,\delta_t}} \; \frac{\left(\frac{\partial c_{h_f}}{\partial \delta_f}\right)_{\alpha,\delta_t} - \left(\frac{\partial C_{h_f}}{\partial \delta_f}\right)_{\alpha,\delta_t}}{\left(\frac{\partial c_{h_f}}{\partial \delta_f}\right)_{\alpha,\delta_t}} \; \frac{\left(\frac{\partial c_{h_f}}{\partial \delta_f}\right)_{\alpha,\delta_t}}{\left(\frac{\partial c_{h_f}}{\partial \delta_t}\right)_{\alpha,\delta_f}}$$

This equation represents the reduction in tab hinge-moment effectiveness resulting from a change from infinite to finite aspect ratio.

For usual tab-flap chord ratios of about 0.2, the data of reference 7 may be used to show that

$$\frac{\left(\frac{\partial \alpha}{\partial \delta_t}\right)_{c_l, \delta_f}}{\left(\frac{\partial \alpha}{\partial \delta_f}\right)_{c_l, \delta_t}} \approx 0.4$$

Table II of reference 21 indicates that for aspect ratios in the vicinity of $A = 6$

$$\frac{\left(\frac{\partial c_{h_f}}{\partial \delta_f}\right)_{\alpha, \delta_t} - \left(\frac{\partial c_{h_f}}{\partial \delta_f}\right)_{\alpha, \delta_t}}{\left(\frac{\partial c_{h_f}}{\partial \delta_f}\right)_{\alpha, \delta_t}} \approx 0.50$$

and figures 142 and 147 of reference 2 indicate that

$$\frac{\left(\frac{\partial c_{h_f}}{\partial \delta_f}\right)_{\alpha, \delta_t}}{\left(\frac{\partial c_{h_f}}{\partial \delta_t}\right)_{\alpha, \delta_f}} \approx 1.0$$

A reduction of about 20 percent can therefore be expected in tab hinge-moment effectiveness when correcting infinite aspect-ratio results to a finite aspect ratio of about 6. The aspect ratios of the model configurations of table I generally vary through only a relatively small range so that the difference resulting from changes in aspect ratio between the values of the tab hinge-moment effectiveness for these models will generally be much less than 20 percent and can be neglected.

For partial-span tabs the effects of aerodynamic induction in reducing the load over the tab and flap are partly compensated by the load induced by the tab on the part of the flap located at the sides of the tab. The aspect-ratio corrections, therefore, are probably greatest for full-span tabs.

The values of $\left(\frac{\partial C_{h_f}}{\partial \delta_t}\right)_{\alpha,\delta_f}$ used in the analysis were, except when otherwise stated, measured at approximately zero angle of attack and flap deflection. These values can be expected to represent the tab effect in a tab-deflection range of approximately ± 10 degrees. When tests were made with the tab linked to the flap, $\left(\frac{\partial C_{h_f}}{\partial \delta_t}\right)_{\alpha,\delta_f}$ was determined by means of the equation already presented for the hinge moments of a flap with a linked tab.

RESULTS AND DISCUSSION

The results of the analysis are presented in two parts as follows: (1) a correlation of the data suitable for quantitative analysis in a form useful for design purposes, and (2) a collection of the remaining data in a form that indicates the direction and general magnitude of the effects resulting from changes in the remaining variables.

Quantitative Analysis

The correlation consisted mainly in the determination of empirical relationships to represent the variation of the tab hinge-moment effectiveness $\left(\frac{\partial C_{h_f}}{\partial \delta_t}\right)_{\alpha,\delta_f}$ with flap and tab chord, with control-surface balance, and with trailing-edge angle. Section data for only one trailing-edge angle were available in sufficient quantity to determine the variation of the tab hinge-moment effectiveness with flap chord. The assumption that this expression applies also to the finite-span data, regardless of trailing-edge angle, made it possible to determine an expression for the variation with trailing-edge angle by iteration. This expression was then assumed to apply also to section data.

Effect of flap chord.- Figure 1 shows data from figure 147 of reference 2 on the variation of the section tab hinge-moment effectiveness with flap-airfoil chord ratio and tab-flap chord ratio. These data are not corrected for the effects of tunnel walls. For the tab-flap chord ratios shown in figure 1, the following empirical expression, which would reduce the family of curves to one basic curve, was determined:

$$K_c' = 1 + 0.51 \left(\frac{c_t}{c_f}\right)^{-0.69} \frac{c_f}{c} \tag{1}$$

Dividing the measured values of the section tab hinge-moment effectiveness by K_c' represents an extrapolation to a basic curve β, which is also shown in figure 1. The variation of the section tab hinge-moment effectiveness for any flap-airfoil chord ratio can now be written

$$\left(\frac{\partial c_{h_f}}{\partial \delta_t}\right)_{\alpha,\delta_f} = K_c'\beta \tag{2}$$

If equation (2) is assumed to apply in three-dimensional flow, the hinge-moment coefficients must be based only on the span of the control surface occupied by the tab and on the root-mean-square chord of this same part of the control surface. The hinge-moment coefficients can be based on these quantities as follows:

$$\left(\frac{\partial C_{h_f}}{\partial \delta_t}\right)_{\alpha,\delta_f} = K_t K_c{}'\beta \tag{3}$$

where

$$K_t = \frac{b_t \bar{c}_f{}'^2}{b_f \bar{c}_f{}^2}$$

Effect of balance.- Because the data of figure 1 apply only to control surfaces without balance, an expression representing the effect of balance must be inserted in equation (3) as follows:

$$\left(\frac{\partial C_{h_f}}{\partial \delta_t}\right)_{\alpha,\delta_f} = K_b K_t K_c{}'\beta \tag{4}$$

where

$$K_b = 1 - \frac{P_{\delta_t}}{2\left(\frac{\partial c_{h_f}}{\partial \delta_t}\right)_{\alpha,\delta_f}} \left[\left(\frac{c_b}{c_f}\right)^2 - \left(\frac{t_f}{2c_f}\right)^2\right]$$

The term $\frac{t_f}{2c_f}$ corrects for that part of the overhang which contributes no balancing moment. The factor $\frac{P_{\delta_t}}{2\left(\frac{\partial c_{h_f}}{\partial \delta_t}\right)_{\alpha,\delta_f}}$ is the ratio of the effective pressure over the balance to a fictitious rectangularly distributed effective pressure over the flap. Calculations based on the pressure distributions of figure 140 of reference 2 showed this ratio to depend primarily on the tab-flap chord ratio. A fairly consistent but rather small variation with flap-airfoil chord ratio was also noticed. In the range of tab-flap chord ratio considered (0.1 to 0.5) a single curve was faired that would represent $\dfrac{P_{\delta_t}}{2\left(\dfrac{\partial c_{h_f}}{\partial \delta_t}\right)_{\alpha,\delta_f}}$ (accurate to about 10 percent) for any flap-airfoil chord ratio. This curve is shown in figure 2, together with test points from force tests of two models. Because the entire term $\left[\left(\dfrac{c_b}{c_f}\right)^2 - \left(\dfrac{t_f}{2c_f}\right)^2\right]$ is usually small compared with 1, evaluation of $\dfrac{P_{\delta_t}}{2\left(\dfrac{\partial c_{h_f}}{\partial \delta_t}\right)_{\alpha,\delta_f}}$ for each tab-flap chord ratio from figure 2 was not considered necessary. The value of 0.85 at $\dfrac{c_t}{c_f} = 0.25$ (approximately the average tab-flap chord ratio of the tabs tested) was used to obtain values of K_b from equation (4).

Determination of trailing-edge-angle factor and revised basic curve from finite-span data.- Reference 5 indicates that the effects of changes in airfoil profile shape on control-surface hinge-moment characteristics can be accounted for largely in terms of the airfoil trailing-edge angle. This result led to the assumption that the effects of changes in airfoil profile shape on the tab hinge-moment effectiveness might also be accounted for largely in terms of the airfoil trailing-edge angle, and a study was therefore made of the available tab data. This study indicated that, for a model under given test conditions, profile modifications increasing the trailing-edge angle caused a decrease in the tab hinge-moment effectiveness. Equation (4) was used to reduce the finite-span tab data for all models to the same nondimensional form, balance chord, and flap chord. From the various trailing-edge angles tested, a factor K_ϕ was determined to account for the variation of tab hinge-moment effectiveness with trailing-edge angle. Equation (4) was then written

$$\left(\frac{\partial c_{h_f}}{\partial \delta_t}\right)_{\alpha, \delta_f} = K_\phi K_b K_t K_c{}' \beta \qquad (5)$$

A comparison of the data and equation (5) showed that the variation of β presented in figure 1 did not represent the available finite-span data; therefore, K_ϕ and B (a revised basic curve) were unknown and had to be determined by iteration. The following empirical expressions resulted:

$$K_\phi = 1.3 - 0.026\phi \qquad (6)$$

$$B = -0.022 \left(\frac{c_t}{c_f}\right)^{0.72} \qquad (7)$$

Plots of these equations, with test points from the available finite-span data, are shown in figures 3 and 4, respectively.

In order to give some indication of the comparison of two-dimensional force-test data with the pressure-distribution data of figure 1, the available force-test data obtained from model configurations described in table II are shown in figure 1. These data were reduced to a form corresponding to the basic curve β. The trailing-edge-angle factor deduced from finite-span data was assumed to apply.

Substituting B for β and inserting the trailing-edge-angle factor permits equation (4) to be written

$$\left(\frac{\partial c_{h_f}}{\partial \delta_t}\right)_{\alpha, \delta_f} = -0.022\ K_\phi K_b K_t K_c{}' \left(\frac{c_t}{c_f}\right)^{0.72} \qquad (8)$$

An examination of the product $K_c' \left(\frac{c_t}{c_f}\right)^{0.72}$, which equals

$$\left[1 + 0.51 \left(\frac{c_t}{c_f}\right)^{-0.69} \frac{c_f}{c}\right] \left(\frac{c_t}{c_f}\right)^{0.72}$$

showed that, if an average of the numerical values of the exponents of c_t/c_f is taken as 0.70, this product can be simplified to

$$K_c = \left(\frac{c_t}{c_f}\right)^{0.70} + 0.51 \left(\frac{c_f}{c}\right)$$

where

$$K_c = K_c' \left(\frac{c_t}{c_f}\right)^{0.70}$$

This approximation was found to be sufficiently accurate; therefore, equation (8) can be written

$$\left(\frac{\partial c_{h_f}}{\partial \delta_t}\right)_{\alpha,\delta_f} = -0.022 K_\phi K_b K_t K_c \frac{q_t}{q} \qquad (9)$$

The ratio q_t/q is inserted to account for any differences that may exist between the dynamic pressure of the air stream in which the tab is located and the dynamic pressure on which the coefficients are based, such as in the case of a tail surface in the propeller slipstream.

Final correlation.- The final correlation of the available tab data based on equation (9) is presented in figure 5, which indicates that the tab hinge-moment effectiveness can be estimated from the geometric characteristics of the tab-flap-airfoil combination by use of equation (9).

The determination of the quantities expressed by equations (6) and (7) was made rather difficult by scatter caused by boundary-layer changes resulting from changes in transition location, flap gap, turbulence, and Reynolds number; furthermore, in every case, insufficient data were available to determine quantitatively the effect of these variables for inclusion in the correlation. For this reason equations (6) and (7) probably do not give the exact magnitude of the effect but, since both equations introduce only relatively small changes from the original pressure-distribution data, they were considered satisfactory. An examination of table I shows that about 90 percent of the available finite-span tab data was for sealed tab gaps. The correlation can therefore be considered as based on the tab-gap-sealed condition.

Special case of thin attached tabs.- Tabs are frequently applied to control surfaces simply by attaching a piece of sheet metal that extends behind the trailing edge. Characteristics of such attached-tab model configurations are included in table I. Values of the flap-airfoil chord ratio and the tab-flap chord ratio are based on airfoil and flap chords extended by the chord of the tab. By use of these values of the flap-airfoil and tab-flap chord ratios with the trailing-edge angle of the airfoil in equation (9), the attached-tab results were found to agree reasonably well with the previous correlation of results for inset tabs as shown in figure 5.

It should be remembered that when an attached tab is applied to a control surface, $\left(\frac{\partial C_{h_f}}{\partial \alpha}\right)_{\delta_f,\delta_t}$ and $\left(\frac{\partial C_{h_f}}{\partial \delta_f}\right)_{\alpha,\delta_t}$ change somewhat as a result of the altered chord and trailing-edge angle.

Flight data.- Flight data are available for several tabs installed on elevators. The characteristics of these tabs are shown in table III. Figure 6 shows data typical of the flight measurements from configuration 2, table III. These data show that as the indicated airspeed decreases, the tab hinge-moment effectiveness increases for climbing flight and decreases for gliding flight - the increase for climbing flight probably resulting from increasing q_t/q caused by the propeller thrust and the decrease in gliding flight resulting from decreasing q_t/q caused by the airplane drag and the windmilling propeller. Values of tab hinge-moment effectiveness to be compared with the correlation were therefore taken at high speeds (for example, 300 mph in fig. 6) where the decrease in q_t/q caused by drag is approximately offset by the increase caused by the propeller so that it can be assumed that $\frac{q_t}{q} = 1$. These values of the tab hinge-moment effectiveness were found to compare favorably with those indicated by equation (9) as shown in the following table:

Configuration	$\left(\frac{\partial C_{h_f}}{\partial \delta_t}\right)_{\alpha,\delta_f}$	
	Equation (9)	Flight
1	-0.0033	-0.0028
2	-.0029	-.0033
3	-.0044	-.0044
4	-.0058	-.0051
5	-.0021	-.0020

Figure 5 shows that the agreement of the flight data with equation (9) is as good as that of the wind-tunnel data.

Qualitative Analysis

The qualitative analysis deals chiefly with the parameters that vary the tab hinge-moment effectiveness by changing the boundary-layer thickness over the tab. The effects of transition location, surface condition, gap at hinges, Reynolds number, turbulence, flap deflection, angle of attack, and compressibility are briefly discussed.

Effect of transition location.- A decreased tab hinge-moment effectiveness would be expected to result from thickening the boundary layer by moving the transition forward. Such a decrease in effectiveness is shown in figure 5 by the available data on transition location. The solid symbols shown correspond to data for the same models as the open symbols of the same shape except that the transition has been moved forward approximately as indicated by table I. These data indicate that with airfoils having surface condition such that transition is at approximately maximum thickness, reductions in the tab hinge-moment effectiveness occur as a result of moving the transition to the vicinity of the leading edge. For airfoils having a well-defined low-drag range a sudden change in the tab hinge-moment effectiveness can therefore be expected at flap deflections and angles of attack corresponding to the limits of the low-drag range.

Effect of surface condition.- Roughness will lead to a decrease in tab hinge-moment effectiveness when its addition causes the transition to move forward. Unpublished data indicate that, even when extensive laminar flow is not realized, an appreciable increase in boundary-layer thickness will result from the addition of roughness in the turbulent boundary layer; consequently, a corresponding decrease in tab hinge-moment effectiveness will occur.

Effects of flap and tab gaps.- The effects on tab characteristics of gap at tab and flap hinges result from a tendency of the flow induced through the gap by tab deflection to change the boundary layer over the tab. The data of reference 3 on the effect of flap gap (fig. 7) indicate that, in the usual range of flap gaps (0 to 0.005c), the tab hinge-moment effectiveness decreases with increasing gap. Figure 140 of reference 2 indicates that the pressure resulting from tab deflection at the tab hinge may be, for tab-flap chord ratios commonly used, three to five times that at the flap hinge. Much larger reductions of the tab hinge-moment effectiveness are therefore to be expected from unsealing the tab gap than from unsealing the flap gap. The only comparable data on the effects of tab gap are obtained from tests of models 11(a) and 11(b) (table I) and show that unsealing a 0.0016c gap reduced the tab hinge-moment effectiveness about 20 percent. Less reliable data indicate the possibility of even larger reductions. Tab gaps obviously should be sealed.

Effect of Reynolds number.- Increasing the Reynolds number has two effects on the boundary layer. First, increasing the Reynolds number tends to thin the boundary layer with the result that the tab hinge-moment effectiveness is increased. Second, as the boundary layer becomes thinner the size of roughness particles or surface irregularities on the airfoil effectively increases relative to the boundary-layer thickness, so that a Reynolds number is reached at which the roughness causes the transition to move forward. This forward movement of the transition with consequent increase in boundary-layer thickness at the trailing edge results in a decreased tab hinge-moment effectiveness. The tab hinge-moment effectiveness may, therefore, either increase or decrease with Reynolds number. Whether an increase or a decrease occurs depends on the range of Reynolds number under consideration and on the surface condition of the airfoil.

Effect of turbulence.- Decreasing the turbulence in the air stream over the tab-flap-airfoil combination tends to result in a more extensive laminar-flow region. A thinner boundary layer over the tab with a corresponding increase in the tab hinge-moment effectiveness can therefore be expected.

Effect of flap deflection and angle of attack.- The tab hinge-moment effectiveness data used thus far in the analysis have been measured at zero flap deflection and approximately zero angle of attack. For control-surface deflections other than zero the tab hinge-moment effectiveness appears to become somewhat discontinuous at $\delta_t = 0^\circ$, with the result that two values of the effectiveness are obtained for each flap deflection - one corresponding to negative and one to positive tab deflections. Figure 8 shows typical variations of two such values of the tab hinge-moment effectiveness with flap deflection and indicates that control-surface deflection decreases the effectiveness of the balancing tab (δ_f and δ_t having opposite signs) and increases the effectiveness of the unbalancing tab (δ_f and δ_t having like signs). The effect shown in figure 8 increased with forward movement of the transition and the corresponding increasing boundary-layer thickness. An investigation of the effect of small angles of attack on the tab hinge-moment effectiveness did not lead to any consistent results. Figure 9, which shows the increment of control-surface hinge-moment coefficient corresponding to positive and negative tab deflections of 10° (reference 10) was included, however, because it indicates that a tab may retain a reasonable part of its hinge-moment effectiveness through and beyond the stall.

Effect of compressibility.- Because of the increased boundary-layer thickness associated with Mach numbers approaching the critical, a decrease in tab hinge-moment effectiveness is probably to be expected as the Mach number increases. Such a decrease is shown for model 20 (table I) in figure 10. Figure 11 shows the variation of hinge-moment coefficient with control-surface deflection for an aileron-tab combination having two linkage ratios and at different Mach numbers. The most important indication of the data of figures 10 and 11 is that a tab may retain a relatively large part of its effectiveness through the subcritical range of Mach number.

DESIGN PROCEDURE

In order to design a tab to produce a desired change in the hinge-moment characteristics of a control surface equation (9), which gives the change in control-surface hinge moment per degree tab deflection, can be used; thus,

$$\left(\frac{\partial C_{h_f}}{\partial \delta_t}\right)_{\alpha,\delta_f} = -0.022\ K_\phi\ K_b\ K_t\ K_c\ \frac{q_t}{q}$$

Figure 12 presents a diagram of a typical tab-flap-airfoil combination, on which are defined the parameters that determine the numerical values of the factors K_ϕ, K_b, K_t and K_c. These parameters may be used to determine K_ϕ from the equation

$$K_\phi = 1.3 - 0.026\phi$$

or from figure 3. The factor K_t is given by

$$K_t = \frac{b_t}{b_f}\left(\frac{\bar{c}_f'}{\bar{\bar{c}}_f}\right)^2$$

and can be evaluated from figure 13(a). The factor K_c is given by

$$K_c = \left(\frac{c_t}{c_f}\right)^{0.70} + 0.51\,\frac{c_f}{c}$$

and can be evaluated from figure 13(b). The factor K_b is given by

$$K_b = 1 - 0.85\left[\left(\frac{c_b}{c_f}\right)^2 - \left(\frac{t_f}{2c_f}\right)^2\right]$$

and can be evaluated from figure 13(c). The factor q_t/q is the ratio of the dynamic pressure of the air stream over the tab to the dynamic pressure on which the hinge-moment coefficients are based.

CONCLUSIONS

The analysis of the available data on the effect of tabs on control-surface hinge moments indicated the following conclusions:

1. The effects of a tab on control-surface hinge moments can be estimated with a reasonable degree of accuracy from geometric characteristics of the tab-flap-airfoil combination.

2. The tab hinge-moment effectiveness is reduced by increasing the trailing-edge angle or by any alteration of the airfoil surface condition or of the air stream, such as moving the transition forward, roughening the surface, or increasing the turbulence, that tends to increase the boundary-layer thickness near the trailing edge.

3. The tab hinge-moment effectiveness may either increase or decrease with Reynolds number. Whether an increase or a decrease occurs depends on the range of Reynolds number under consideration and on the surface condition of the airfoil.

4. Gaps at flap and tab hinges reduce the tab hinge-moment effectiveness and the reduction resulting from tab gap generally is so large as to make seals advisable.

5. A reasonable part of the tab hinge-moment effectiveness may prevail through and beyond the stall.

6. The tab hinge-moment effectiveness decreases with control-surface deflection for a balancing tab and increases with deflection for an unbalancing tab.

7. Increasing the Mach number probably decreases the tab hinge-moment effectiveness; however, a relatively large part of the effectiveness may be retained through the subcritical range of Mach number.

Langley Memorial Aeronautical Laboratory
National Advisory Committee for Aeronautics
Langley Field, Va., April 22, 1946

REFERENCES.

1. Rogallo, F. M.: Collection of Balanced-Aileron Test Data. NACA ACR No. 4A11, 1944.

2. Sears, Richard I.: Wind-Tunnel Data on the Aerodynamic Characteristics of Airplane Control Surfaces. NACA ACR No. 3L08, 1943.

3. Rogallo, F. M., and Lowry, John G.: Résumé of Data for Internally Balanced Ailerons. NACA RB, March 1943.

4. Purser, Paul E., and Toll, Thomas A.: Analysis of Available Data on Control Surfaces Having Plain-Overhang and Frise Balances. NACA ACR No. L4E13, 1944.

5. Purser, Paul E., and Gillis, Clarence L.: Preliminary Correlation of the Effects of Beveled Trailing Edges on the Hinge-Moment Characteristics of Control Surfaces. NACA CB No. 3E14, 1943.

6. Lowry, John G.: Résumé of Hinge-Moment Data for Unshielded Horn-Balanced Control Surfaces. NACA RB No. 3F19, 1943.

7. Swanson, Robert S., and Crandall, Stewart M.: Analysis of Available Data on the Effectiveness of Ailerons without Exposed Overhang Balance. NACA ACR No. L4E01, 1944.

8. Sears, Richard I.: Wind-Tunnel Investigation of Control-Surface Characteristics. I - Effect of Gap on the Aerodynamic Characteristics of an NACA 0009 Airfoil with a 30-Percent-Chord Plain Flap. NACA ARR, June 1941.

9. Sears, Richard I., and Liddell, Robert B.: Wind-Tunnel Investigation of Control-Surface Characteristics. VI - A 30-Percent-Chord Plain Flap on the NACA 0015 Airfoil. NACA ARR, June 1942.

10. Gillis, Clarence L., and Lockwood, Vernard E.: Wind-Tunnel Investigation of Control-Surface Characteristics. XIII - Various Flap Overhangs Used with a 30-Percent-Chord Flap on an NACA 66-009 Airfoil. NACA ACR No. 3G20, 1943.

11. Harris, Thomas A.: Reduction of Hinge Moments of Airplane Control Surfaces by Tabs. NACA Rep. No. 528, 1935.

12. Rogallo, F. M., and Lowry, John G.: Wind-Tunnel Development of Ailerons for the Curtiss XP-60 Airplane. NACA ACR, Sept. 1942.

13. Rogallo, F. M., and Crandall, Stewart M.: Wind-Tunnel Investigation of Trimming Tabs on a Thickened and Beveled Aileron on a Tapered Low-Drag Wing. NACA ACR, March 1943.

14. Sears, Richard I., and Hoggard, H. Page, Jr.: Characteristics of Plain and Balanced Elevators on a Typical Pursuit Fuselage at Attitudes Simulating Normal-Flight and Spin Conditions. NACA ARR, March 1942.

15. Garner, I. Elizabeth: Wind-Tunnel Investigation of Control-Surface Characteristics. XX - Plain and Balanced Flaps on an NACA 0009 Rectangular Semispan Tail Surface. NACA ARR No. L4I11f, 1944.

16. Lowry, John G., Maloney, James A., and Garner, I. Elizabeth: Wind-Tunnel Investigation of Shielded Horn Balances and Tabs on a 0.7-Scale Model of XF6F Vertical Tail Surface. NACA ACR No. 4C11, 1944.

17. Purser, Paul E., and McKee, John W.: Wind-Tunnel Investigation of a Plain Aileron with Thickened and Beveled Trailing Edges on a Tapered Low-Drag Wing. NACA ACR, Jan. 1943.

18. Rogallo, F. M., and Purser, Paul E.: Wind-Tunnel Investigation of a Plain Aileron with Various Trailing-Edge Modifications on a Tapered Wing. III - Ailerons with Simple and Spring-Linked Balancing Tabs. NACA ARR, Jan. 1943.

19. Bryant, L. W., Burge, C. H., Sweeting, N. E., and Greening, J. R.: Experiments on the Balancing of Ailerons by Geared Tabs and Trailing Edge Strips. 5044, S. & C. 1195a, British A.R.C., April 5, 1941.

20. Phillips, W. H., and Nissen, J. M.: Flight Tests of Various Tail Modifications on the Brewster XSBA-1 Airplane. I - Measurements of Flying Qualities with Original Tail Surfaces. NACA ARR No. 3F07, 1943.

21. Swanson, Robert S., and Gillis, Clarence L.: Limitations of Lifting-Line Theory for Estimation of Aileron Hinge-Moment Characteristics. NACA CB No. 3L02, 1943.

TABLE 1.- SUPPLEMENTARY INFORMATION REGARDING WIND-TUNNEL TESTS OF FINITE-SPAN MODELS

[Designations of NACA 6-series airfoils are changed throughout to the present standard NACA form and may therefore be different from the form in which they appear in the references.]

Model: Designation	Model: Symbol	A	λ	Airfoil section	Published reference	Airflow characteristics	Gaps: Control	Gaps: Tab	Type of balance	Transition location	Control location: $\frac{y_1}{b/2}$	Control location: $\frac{y_2}{b/2}$	Tab location: $\frac{y_3}{b_f}$	Tab location: $\frac{y_4}{b_f}$	$\frac{c_t}{c_f}$	$\frac{c_f}{c}$	$\frac{c_b}{c_f}$	$\frac{t_f}{2c_f}$	ϕ (deg)	K_t
Inset tabs																				
1a 1b 1c 1d 1e 1f 1g	○	6.0 ↓	1.00 ↓	Clark Y ↓	1, 12 1, 12 12 ↓ 1, 12	$R = 0.6 \times 10^6$ $M = 0.11$ $\tau = 1.4$	Unsealed ↓	Sealed ↓	None None Frise None ↓	Free ↓	0.700 ↓ .600	1.000 ↓	0 0 .250 .500 0 .250 0	1.000 1.000 .750 1.000 .500 .750 1.000	0.100 .200 ↓ .100	0.400 ↓ .250	0.095 .095 .330 .095 ↓	0.095 ↓	13.0 ↓	1.000 1.000 .500 ↓ 1.000
2a 2b 2c 2d 2e 2f	△	5.6 ↓	0.52 ↓	Root, NACA 66(215)-2(13.716) Tip, NACA 66(215)-2(13.125)	1 1 1, 18 1, 14 14 1, 14	$R = 2.4 \times 10^6$ $M = 0.11$ $\tau = 1.6$	Sealed Unsealed Sealed ↓	Sealed ↓	Internal Frise None ↓	Free ↓	0.264 ↓	0.974 ↓ .900 ↓	0 ↓	0.156 ↓ .300 .200 .200	0.190 ↓ .150 .300 .500	0.200 ↓	0.505 .400 .160 ↓	0.160 ↓	15.0 15.0 31.0 ↓	0.216 ↓ .388 .270 .270
3a 3b 3c	□	6.2 ↓	0.33 ↓	Root, NACA 66,2-118 Tip, NACA 66(2 × 15)-116	13 ↓	$R = 1.9 \times 10^6$ $M = 0.11$ $\tau = 1.6$	Sealed ↓	Sealed ↓	Internal ↓	Free ↓	0.496 ↓	0.894 .894 .940	0 ↓	1.000 .500 .509	0.260 .239 .260	0.149 .162 .149	0.688 .563 .688	0.195 .200 .195	9.0 ↓	0.950 .399 .376
4a 4b 4c 4d 4e 4f	▽	5.6 ↓	0.60 ↓	Root, NACA 23015 5 (approx.) Tip, NACA 23008.25 (approx.)	1, 19 ↓	$R = 1.5 \times 10^6$ $M = 0.08$ $\tau = 1.6$	Sealed ↓	Sealed ↓	None ↓	Free ↓	0.579 ↓	0.984 ↓	0 0 .667 .333 0 0	1.000 .333 1.000 .667 1.000 .667	0.200 ↓	0.155 ↓	0.110 .124 .095 .110 .102 .117	0.110 .124 .095 .110 .102 .117	11.7 13.1 10.2 11.7 10.9 12.3	1.000 .383 .289 .333 .625 .725
5a 5b 5c 5d	◇	4.3 ↓	Elliptic ↓	Root, NACA 2213 Tip, NACA 2205	1, 20 ↓	$R = 1.3 \times 10^6$ $M = 0.06$ τ, unknown	Unsealed ↓	Sealed ↓	None ↓	Free ↓	0.190 ↓	0.793 ↓	0 ↓	0.858 .858 .433 .433	0.158 .329 .176 .324	0.220 ↓	0.122 .122 .127 .127	0.122 .122 .127 .127	12.8 12.8 13.4 13.4	0.962 .962 .621 .621
6	◠	7.2	0.60	------------------------	None	$R = (5.0 \text{ to } 8.4) \times 10^6$ $M = 0.30 \text{ to } 0.73$ $\tau \longrightarrow 1.0$	Unsealed	Sealed	Blunt nose	Free	0.925	0.143	0	0.346	0.376	0.167	0.410	0.158	14.5	0.345
7	◠	7.6	1.00	NACA 43012	None	$R = 2.5 \times 10^6$ $M = 0.16$ $\tau \longrightarrow 1.0$	Unsealed	Sealed	Frise	Free	0.422	0.892	0.355	0.645	0.25	0.188	0.330	0.130	14.5	0.291
8a 8b	▽	10.8 10.8	0.26 .26	Root, NACA 0015 Tip, NACA 0009	None None	$R = 8.9 \times 10^6$ $M = 0.175$ $\tau \longrightarrow 1.0$	Sealed Sealed	Sealed Sealed	Internal Internal	Free Free	0.564 .564	0.965 .965	0.011 .011	0.254 .496	0.236 .236	0.121 .130	0.365 .365	0.145 .145	10.4 10.4	0.245 .435

see errata

NATIONAL ADVISORY COMMITTEE FOR AERONAUTICS

TABLE I.- SUPPLEMENTARY INFORMATION REGARDING WIND-TUNNEL TESTS OF FINITE-SPAN MODELS - Concluded

[Designations of NACA 6-series airfoils are changed throughout to the present standard NACA form and may therefore be different from the form in which they appear in the references.]

Model: Designation	Model: Symbol	A	λ	Airfoil section	Published reference	Airflow characteristics	Gaps: Control	Gaps: Tab	Type of balance	Transition location	Control location: $\frac{y_1}{b/2}$	Control location: $\frac{y_2}{b/2}$	Tab location: $\frac{y_3}{b_f}$	Tab location: $\frac{y_4}{b_f}$	$\frac{c_t}{c_f}$	$\frac{c_f}{c}$	$\frac{c_b}{c_f}$	$\frac{t_f}{2c_f}$	ϕ (deg)	K_t
Inset tabs																				
9a 9b 9c 9d	◁ ◁ ◁ ◁	3.0 ↓ 1.5	0.64 ↓	NACA 0006 ↓	12 ↓	R = 1.2 × 10^6 M = 0.08 τ = 1.4	Unsealed ↓	Sealed ↓	None ↓	Free ↓	0 ↓	1.000 ↓	0 ↓	0.686 ↓	0.10 .20 ↓	0.385 .385 .564 .564	0.063 .063 .054 .054	0.063 .063 .054 .054	7.0 ↓	0.794 ↓
10a 10b	▽ ▽	3.9 3.9	0.58 .58	---------- ----------	None None	R = 2.0 × 10^6 M = 0.11 τ = 1.6	Unsealed Sealed	Sealed Sealed	Blunt nose Blunt nose	Free Free	0.040 .040	0.953 .953	0.150 .094	0.342 .829	0.20 .35	0.491 .340	0.260 .500	0.095 .095	8.2 7.3	0.282 .962
11a 11b	□ □	2.9 2.9	0.39 .39	NACA 16-series modified	17 17	R = 2.3 × 10^6 M = 0.08 τ = 1.6	Sealed Sealed	Sealed Unsealed	None None	Free Free	0 0	1.000 1.000	0.343 .343	0.554 .554	0.30 .30	0.318 .318	0.152 .152	0.152 .152	14.1 14.1	0.225 .225
12a 12b 12c	▷ ▷ ▷	3.7 ↓	0.57 ↓	NACA 0009 ↓	15 ↓	R = 0.5 × 10^6 M = 0.11 τ = 1.6	Sealed ↓	Sealed ↓	None Blunt nose Blunt nose	Free ↓	0 ↓	1.000 ↓	0.195 ↓	0.834 ↓	0.20 ↓	0.306 ↓	0.093 .350 .500	0.093 ↓	11.6 ↓	0.834 ↓
13	△	3.1	1.00	NACA 0014	None	R = 1.0 × 10^6 M = 0.11 τ = 1.6	Sealed	Sealed	Blunt nose	Free	0	0.669	0	0.586	0.410	0.310	0.280	0.125	16.1	0.585
14	◇	2.0	1.00	NACA 0020	None	R = 1.0 × 10^6 M = 0.05	Sealed	Sealed	None	Free	0	0.300	0	1.000	0.200	0.400	0	0.223	25.6	1.000
15	○	3.0	1.00	NACA 0009	16	R = 1.43 × 10^6 M = 0.10 τ = 1.9	Sealed	Sealed	None	Free	0	1.000	0.193	0.679	0.200	0.300	0.093	0.093	11.6	0.486
16	◇	5.5	0.33	NACA 0015	None	----------	Sealed	Unsealed	Internal	Free	0.202	1.000	0	0.605	0.20	0.382	0.558	0.142	19.4	0.804
17a 17b	○ ●	2.17 2.17	0.56 .56	NACA 65(012)-011 modified	None None	R = 3.3 × 10^6 M = 0.21 τ ⟶ 1.0	Sealed Sealed	Unsealed Unsealed	Internal Internal	Free 0.50c Fixed 0.20c	0.238 .238	0.932 .932	0 0	0.533 .533	0.209 .209	0.35 .35	0.325 .325	0.12 .12	14.0 14.0	0.570 .570
18a 18b	▷ ▶	5.0 5.0	0.50 .50	NACA 65_1-012 modified	None None	R = 2.76 × 10^6 M = 0.21 τ ⟶ 1.0	Sealed Sealed	Unsealed Unsealed	Internal Internal	Free 0.50c Fixed 0.25c	0.094 .094	0.943 .943	0 0	0.413 .413	0.20 .20	0.32 .32	0.41 .41	0.131 .131	16.0 16.0	0.545 .545
19a 19b	△ ▲	2.4 2.4	0.50 .50	NACA 0009 NACA 0009	None None	R = 1.9 × 10^6 M = 0.40 τ ⟶ 1.0	Unsealed Unsealed	Unsealed Unsealed	Blunt nose Blunt nose	Free Fixed 0.20c	0 0	1.000 1.000	0.141 .141	0.340 .340	0.25 .25	0.25 .25	0.36 .36	0.10 .10	19.0 19.0	0.255 .255
20	▽	4.5	0.57	----------	None	R = (3.0 to 5.4) × 10^6 M = 0.133 to 0.720 τ ⟶ 1.0	Sealed	Unsealed	Internal	Free	0	0.907	0.206	0.550	0.185	0.55	0.44	0.157	14.9	0.347
21a 21b 21c	◁ ◁ ◁	4.6 ↓	0.50 ↓	Root, NACA 2416 Tip, NACA 4412	None ↓	R = 3.38 × 10^6 M = 0.21 τ ⟶ 1.0	Sealed ↓	Unsealed ↓	Internal ↓	Free 0.25c Fixed 0.0c Free 0.25c	0.167 ↓	0.950 ↓	0 0 .242	0.242 .242 .348	0.25 ↓	0.20 ↓	0.41 ↓	0.17 ↓	19.0 ↓	0.295 .292 .118
Attached tabs																				
22a 22b 22c 22d 22e 22f	○ ○ ○ ○ ○ ○	6.0 ↓	1.00 ↓	Clark Y ↓	12 ↓	R = 0.6 × 10^6 M = 0.11 τ = 1.4	Unsealed ↓	Sealed ↓	None ↓	Free ↓	0.700 ↓	1.000 ↓	0 0 .500 .250 0 0	1.000 ↓ .750 .500 1.000	0.091 .167 ↓ .231	0.423 .444 ↓ .464	0.095 ↓	0.095 ↓	13.0 ↓	1.21 1.44 .72 .72 .72 1.69
23	○	5.6	0.52	Root, NACA 66(215)-2(13.716) Tip, NACA 66(215)-2(13.125)	1, 14	R = 2.4 × 10^6 M = 0.11 τ = 1.6	Unsealed	Sealed	None	Free	0.264	0.900	0	0.126	0.66	0.211	0.160	0.160	31.0	0.21

See errata

NATIONAL ADVISORY
COMMITTEE FOR AERONAUTICS

TABLE II.- SUPPLEMENTARY INFORMATION REGARDING WIND-TUNNEL TESTS OF SECTION MODELS

Model Designation	Model Symbol	A	λ	Airfoil section	Published reference	Airflow characteristics	Gaps Control	Gaps Tab	Type of balance	Transition location	Control location $\frac{y_1}{b/2}$	Control location $\frac{y_2}{b/2}$	Tab location $\frac{y_3}{b_f}$	Tab location $\frac{y_4}{b_f}$	$\frac{c_t}{c_f}$	$\frac{c_f}{c}$	$\frac{c_b}{c_f}$	$\frac{t_f}{2c_f}$	ϕ (deg)	K_b
Inset tabs																				
1	○	∞	1.00	NACA 0009	8	$R = 1.43 \times 10^6$ $M = 0.10$ $T = 1.9$	Sealed	Unsealed	None	Free	0	1.000	0	1.000	0.20	0.30	0.093	0.093	11.6	1.00
2	◇	∞	1.00	NACA 0015	9	$R = 1.43 \times 10^6$ $M = 0.10$ $T = 1.9$	Sealed	Sealed	None	Free	0	1.000	0	1.000	0.20	0.30	0.093	0.093	19.4	1.00
3	◇	∞	1.00	NACA 66-009	10	$R = 1.43 \times 10^6$ $M = 0.10$ $T = 1.9$	Unsealed	Unsealed	None	Free	0	1.000	0	1.000	0.20	0.30	0.093	0.093	6.0	1.00
4	○	∞	1.00	NACA 66(215)-216 a = 0.6	1	$R = (6.7 \text{ to } 9.0) \times 10^6$ $M = 0.24 \text{ to } 0.34$ $T \longrightarrow 1.0$	Sealed	Unsealed	None	Free	0	1.000	0	1.000	0.20	0.2	0.093	0.093	22.0	1.00
5	△	∞	1.00	NACA 65,3-018 modified	None	$R = 2.8 \times 10^6$ $M = 0.20$ $T \longrightarrow 1.0$	Sealed	Sealed	Internal	Free	0	1.000	0	1.000	0.25	0.182	0.406	0.030	25.0	1.00
6	▷	∞	1.00	NACA 2210 modified	None	$R = 3.7 \times 10^6$ $M = 0.20$ $T \longrightarrow 1.0$	Sealed	Sealed	Frise	Free	0	1.000	0	1.000	0.30	0.198	0.294	0.121	25.0	1.00

TABLE III.- SUPPLEMENTARY INFORMATION REGARDING FLIGHT-TEST CONFIGURATIONS

Model Designation	Model Symbol	A	λ	Published reference	Airflow characteristics	Gaps Control	Gaps Tab	Type of balance	Transition location	Control location $\frac{y_1}{b/2}$	Control location $\frac{y_2}{b/2}$	Tab location $\frac{y_3}{b_f}$	Tab location $\frac{y_4}{b_f}$	$\frac{c_t}{c_f}$	$\frac{c_f}{c}$	$\frac{c_b}{c_f}$	$\frac{t_f}{2c_f}$	ϕ (deg)	K_b
Inset tabs																			
1	○	3.5	0.56	21	$R = 8.4 \times 10^6$ $M = 0.290$	Unsealed	Sealed	Horn	Free	0.060	1.000	0.225	0.507	0.186	0.482	0.172	0.172	22.0	0.583
2	6	4.4	0.50	None	$R = 1.2 \times 10^7$ $M = 0.44$	Unsealed	Unsealed	Blunt nose	Free	0.050	1.000	0.252	0.500	0.25	0.34	0.280	0.115	21.0	0.326
3	○	3.5	0.42	None	$R = 8.4 \times 10^6$ $M = 0.29$	Unsealed	Sealed[a]	None	Free	0.060	1.000	0.270	0.555	0.38	0.24	0.129	0.129	20.0	0.400
4	◇	4.9	0.38	None	$R = 14.7 \times 10^6$ $M = 0.40$	Unsealed	Unsealed	None	Free	0.080	1.000	0	0.378	0.255	0.360	0.189	0.189	15.0	0.540
5	◊	3.5	0.49	None	$R = 18.3 \times 10^6$ $M = 0.40$	Unsealed	Unsealed	Blunt nose	Free	0.040	1.000	0.189	0.462	0.286	0.214	0.280	0.105	12.0	0.197

Lsee errata

NATIONAL ADVISORY
COMMITTEE FOR AERONAUTICS

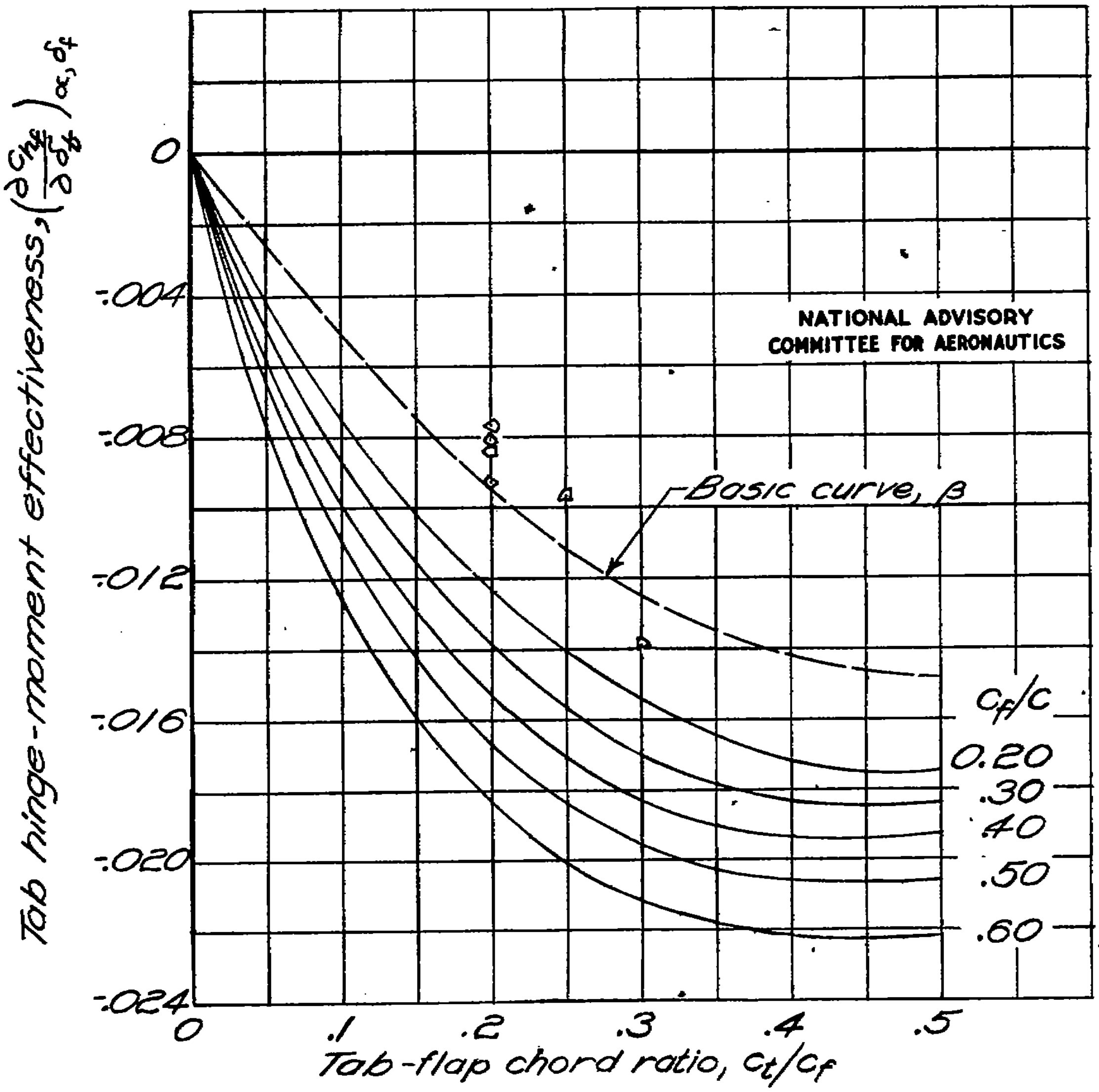

Figure 1.- Variation of tab hinge-moment effectiveness with tab-flap chord ratio as deduced from section pressure-distribution tests with points from section force tests reduced to a form corresponding to the basic curve. Symbols identify models of table II. Data from reference 2.

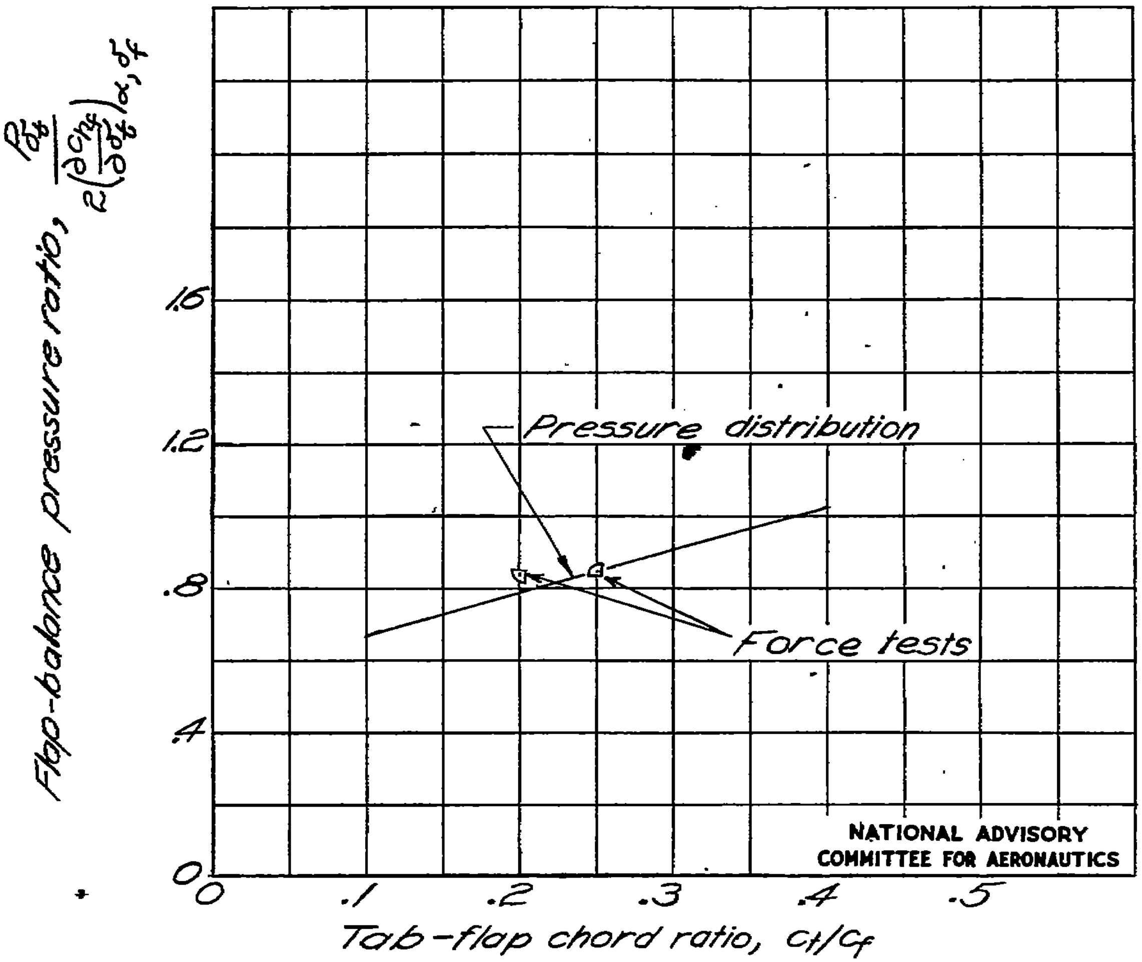

Figure 2.- Effect of tabs on the resultant pressure over a control-surface balance. Symbols identify models of tables I and II.

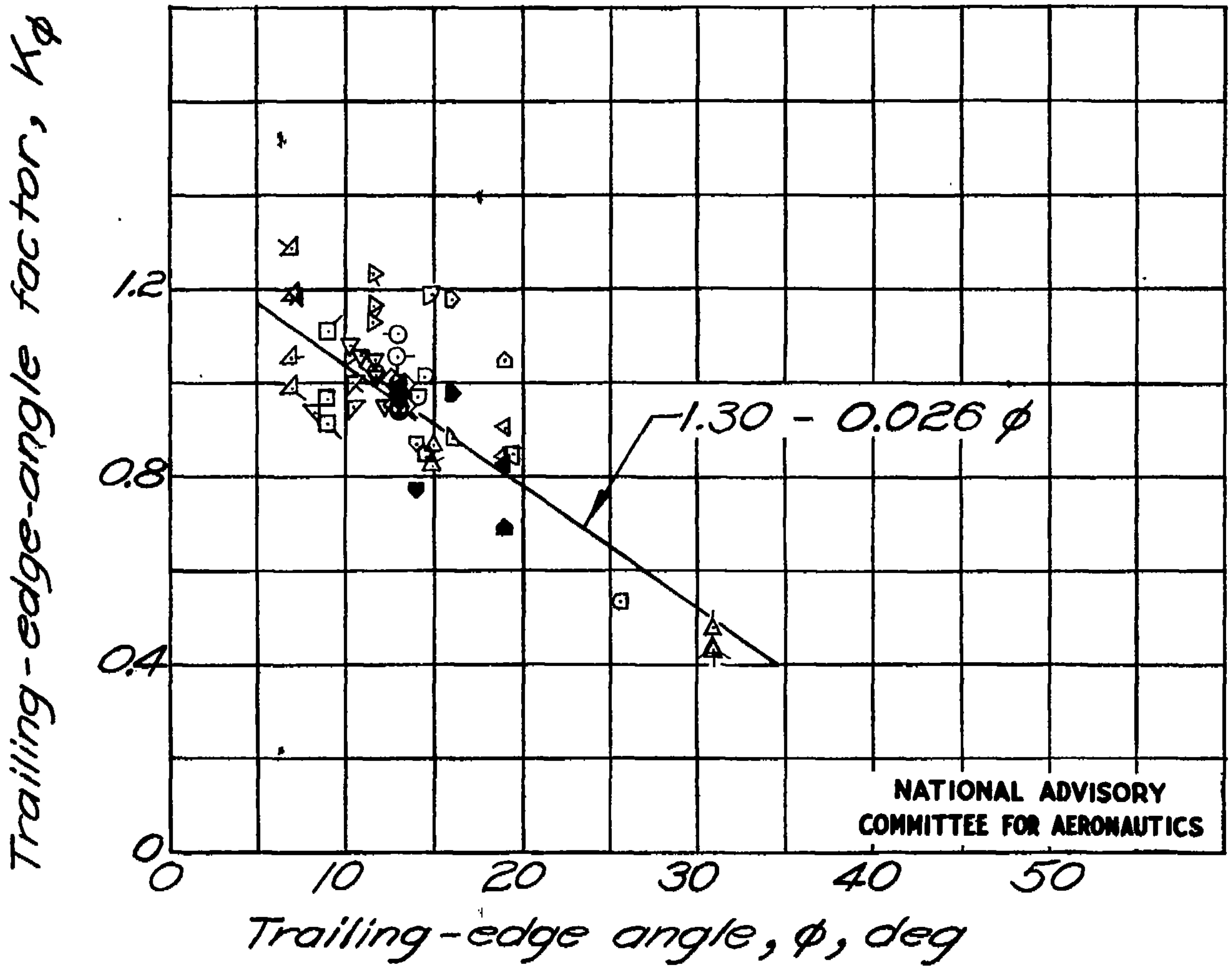

Figure 3.- Effect of trailing-edge angle on the tab hinge-moment effectiveness. Symbols identify models of table I.

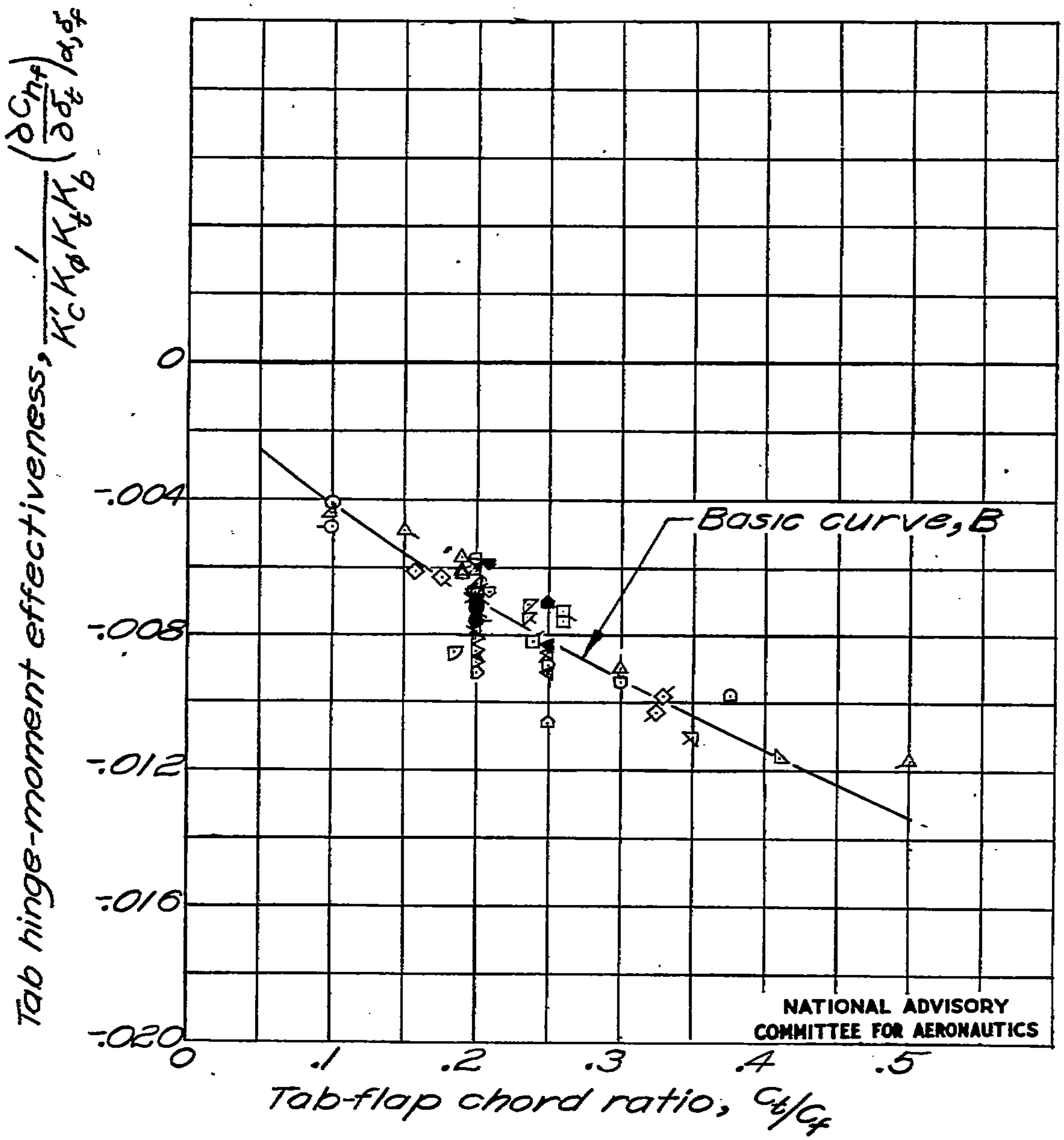

Figure 4.- Variation of tab hinge-moment effectiveness with tab-flap chord ratio as deduced from finite-span force tests. Symbols identify models of table I.

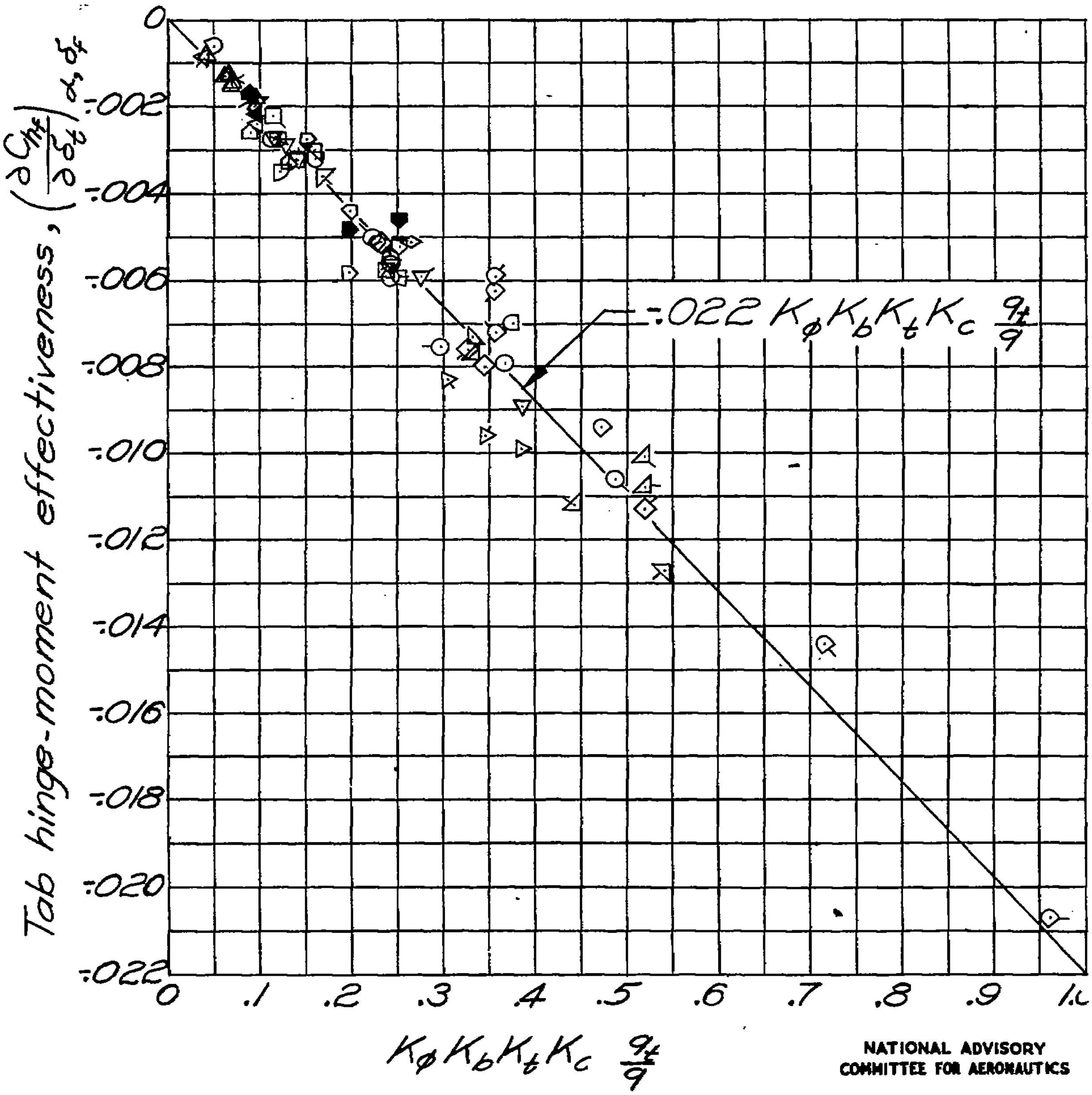

NATIONAL ADVISORY COMMITTEE FOR AERONAUTICS

Figure 5.- Correlation of finite-span-tab hinge-moment effectiveness based on geometric characteristics of the tab-flap-airfoil combination. Symbols identify models of tables I and III.

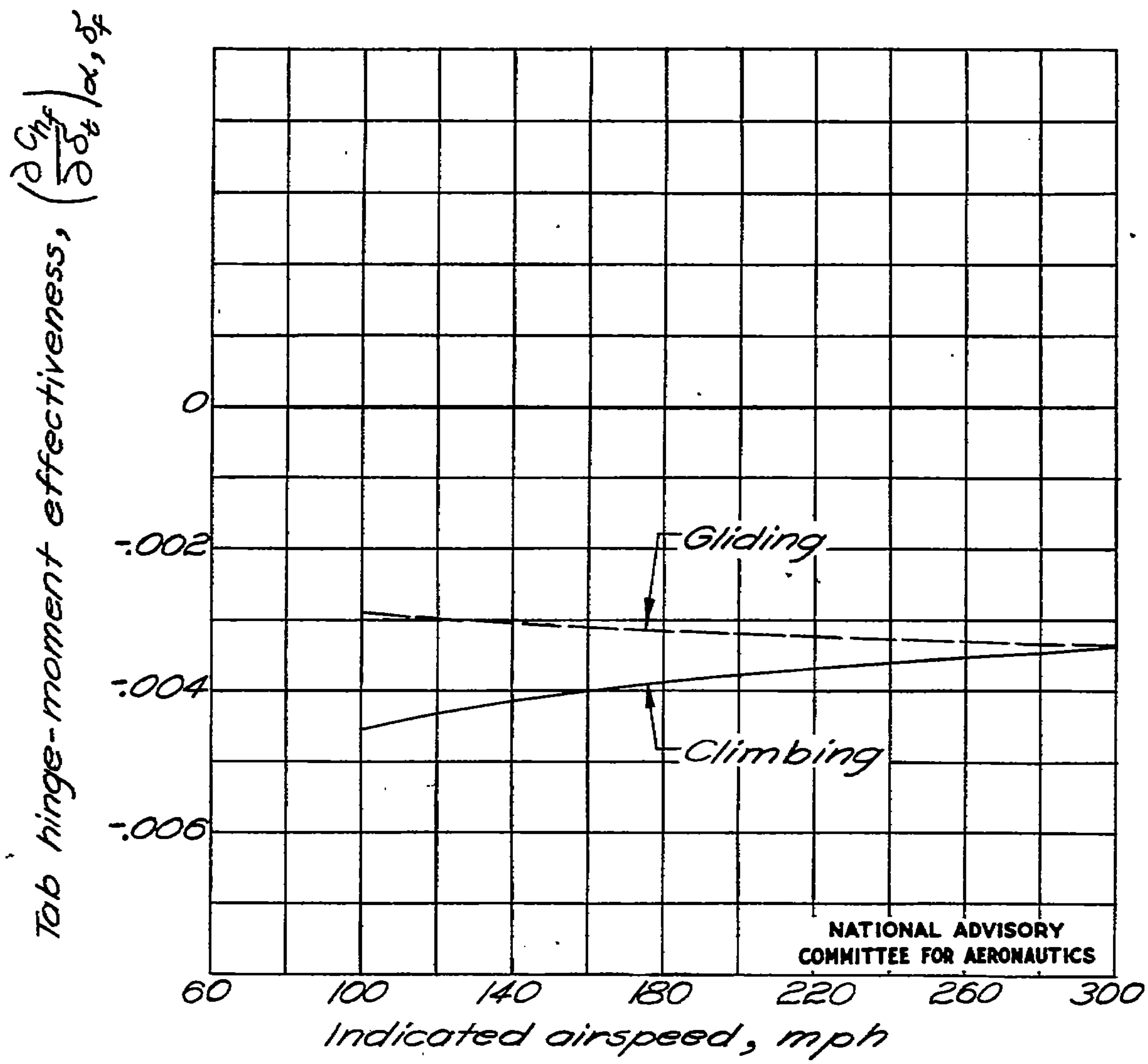

Figure 6.- Tab hinge-moment effectiveness as measured in flight for a tab on the elevator of a fighter-type airplane. Configuration 2, table III.

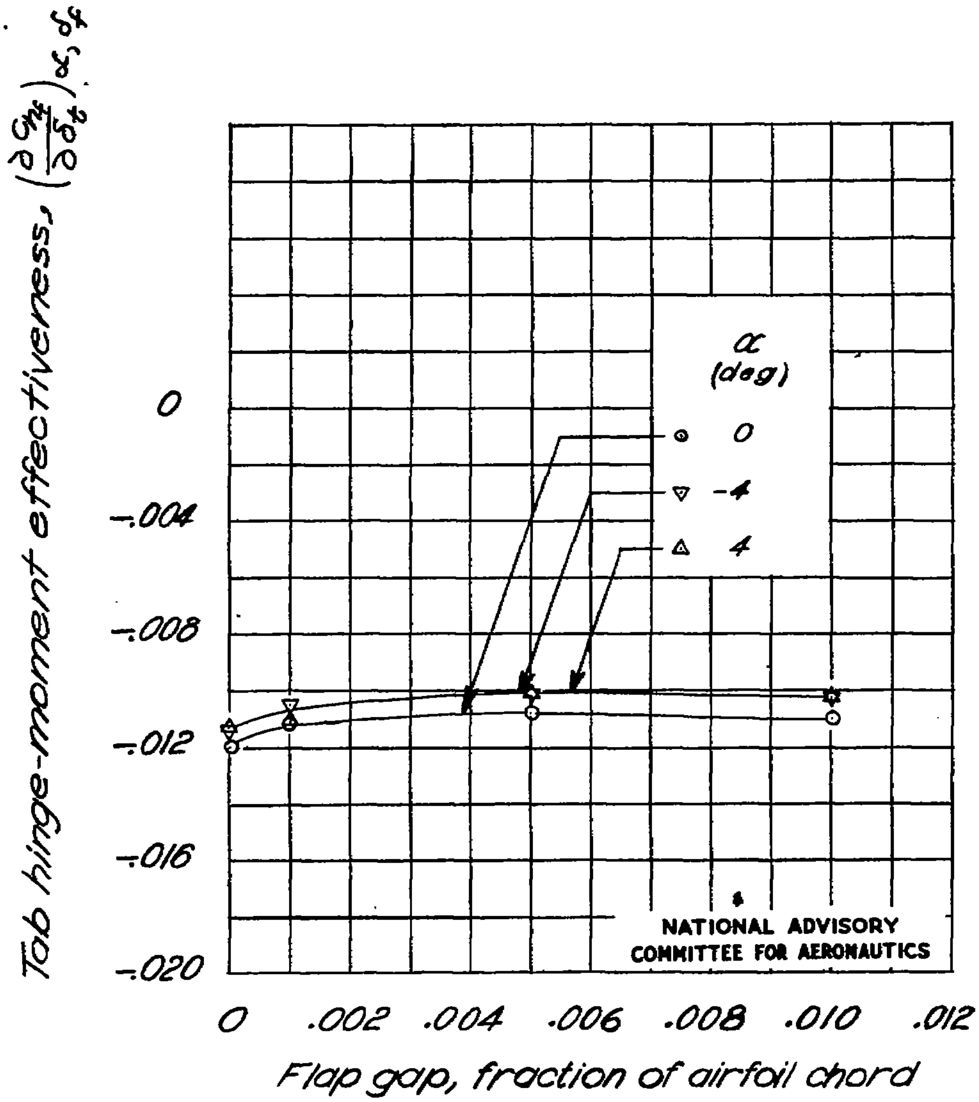

Figure 7.- Effect of flap gap on the hinge-moment effectiveness of $0.20c_f$ tab on a 0.30c plain flap on an NACA 0009 section; tab gap, 0.001c (reference 3).

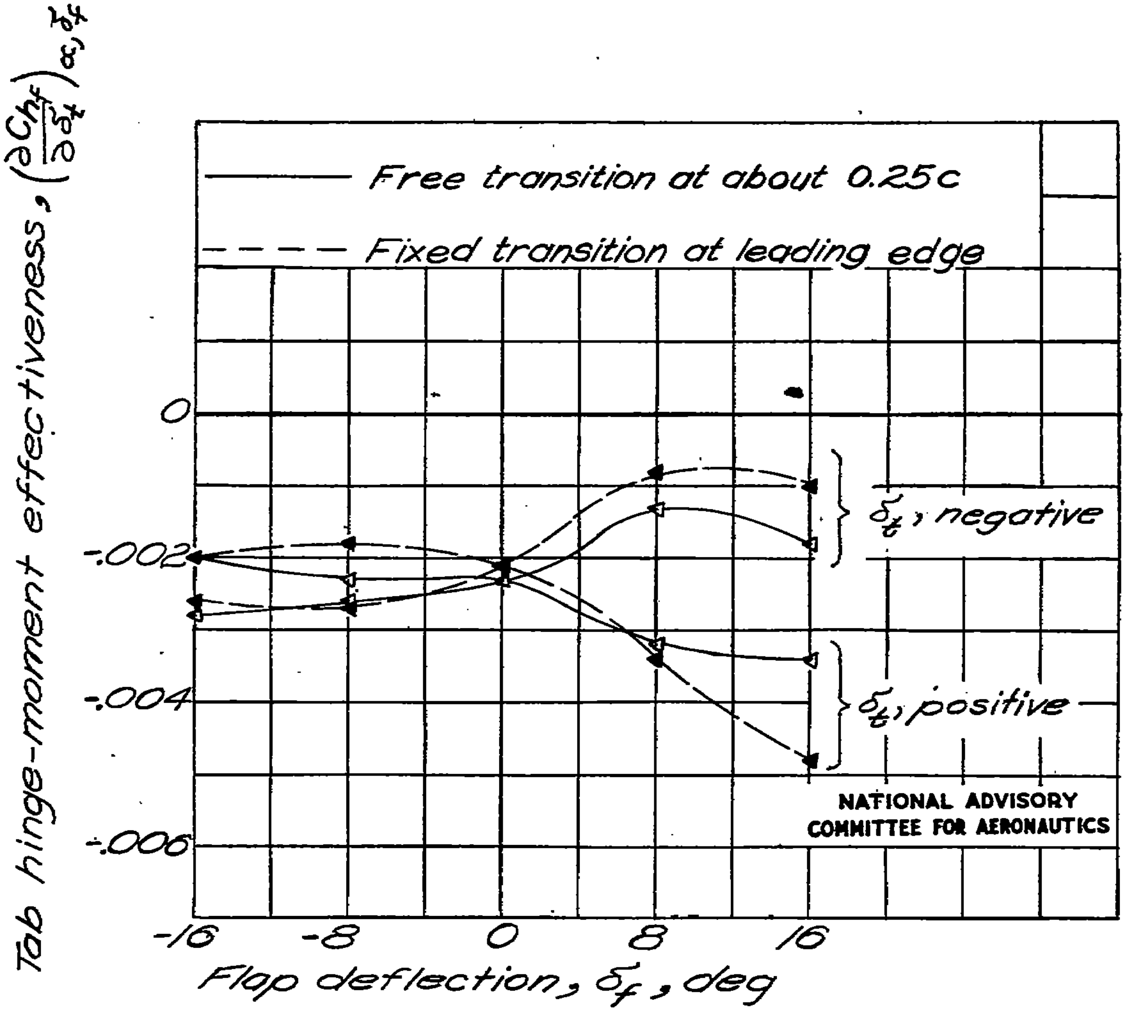

Figure 8.- Effect of flap deflection on the tab hinge-moment effectiveness for two transition locations; α, 0°; models 21a and 21b.

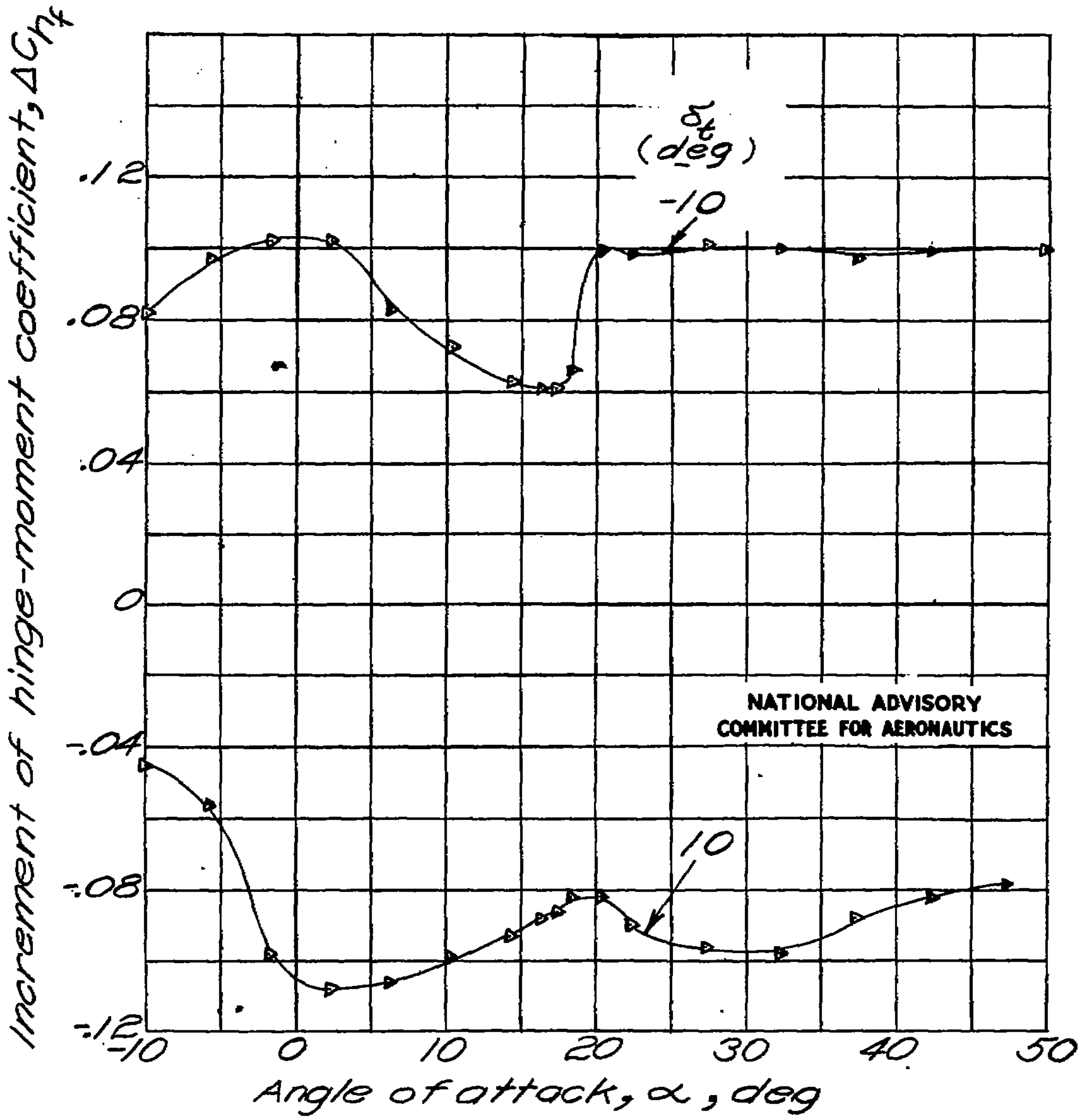

Figure 9.- Variation with angle of attack of the increment of flap hinge-moment coefficient resulting from ±10° tab deflection; $\delta_f = 0°$ (reference 10).

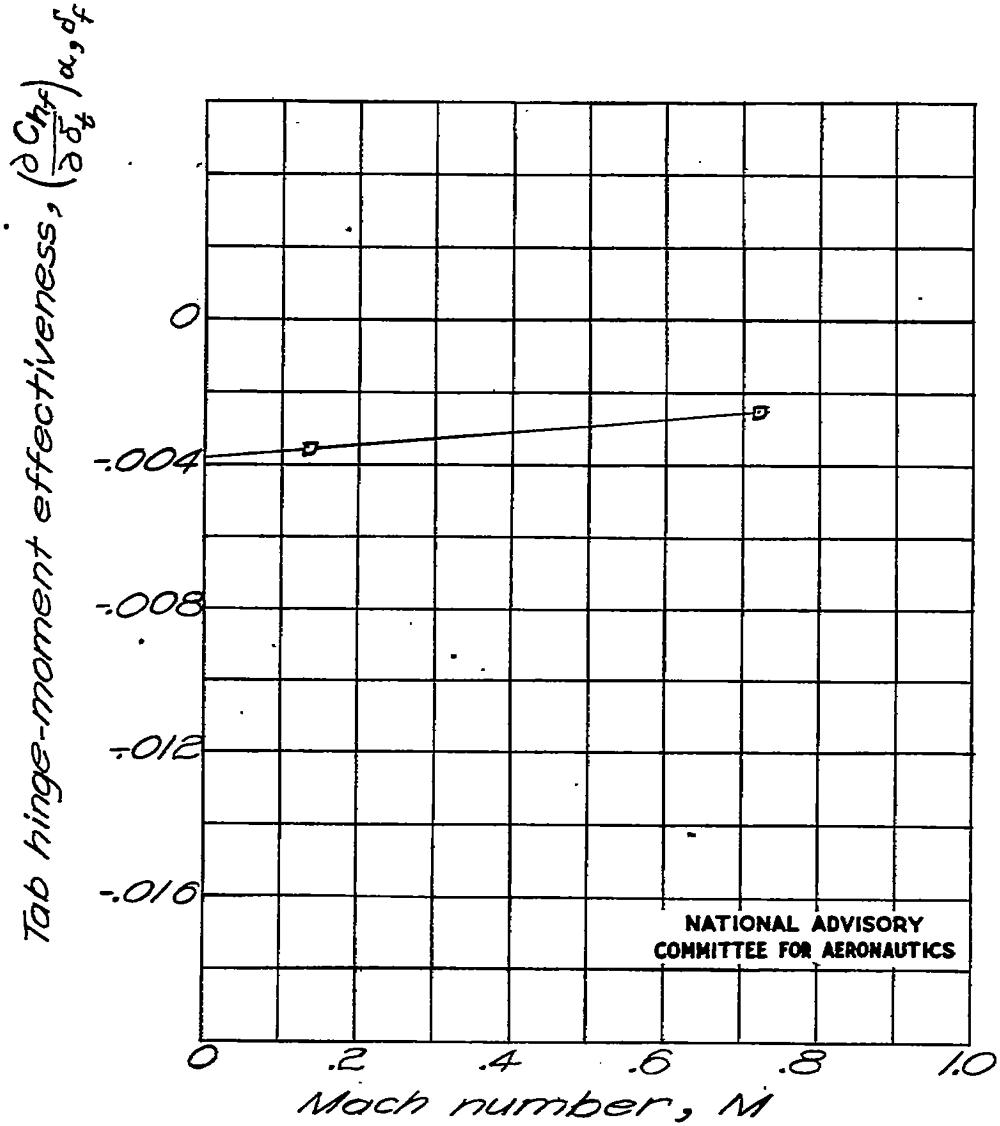

Figure 10. - Variation of tab hinge-moment effectiveness with Mach number; model 20.

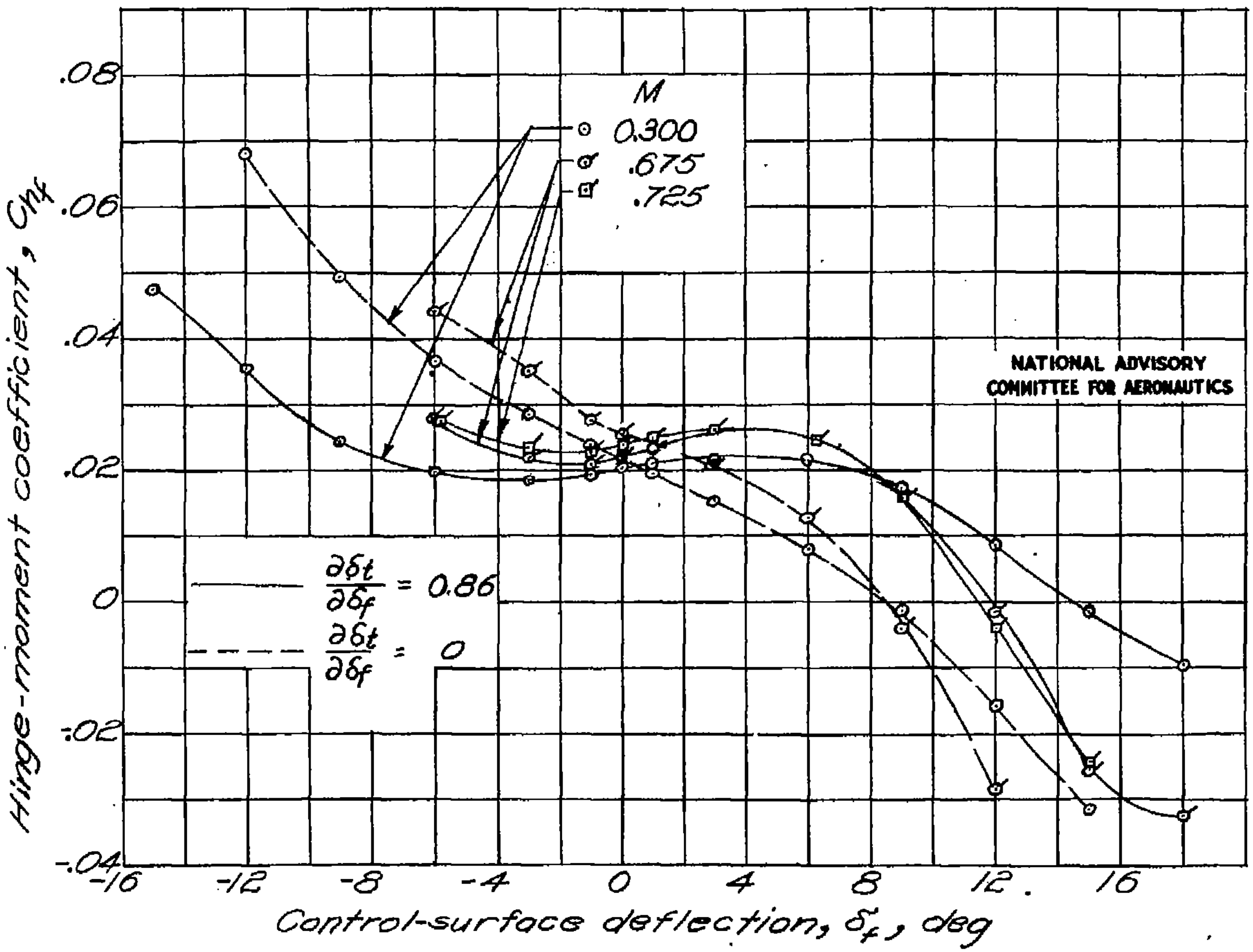

Figure 11. - Variation of control-surface hinge-moment coefficient with Mach number and tab-flap deflection ratio; model 6.

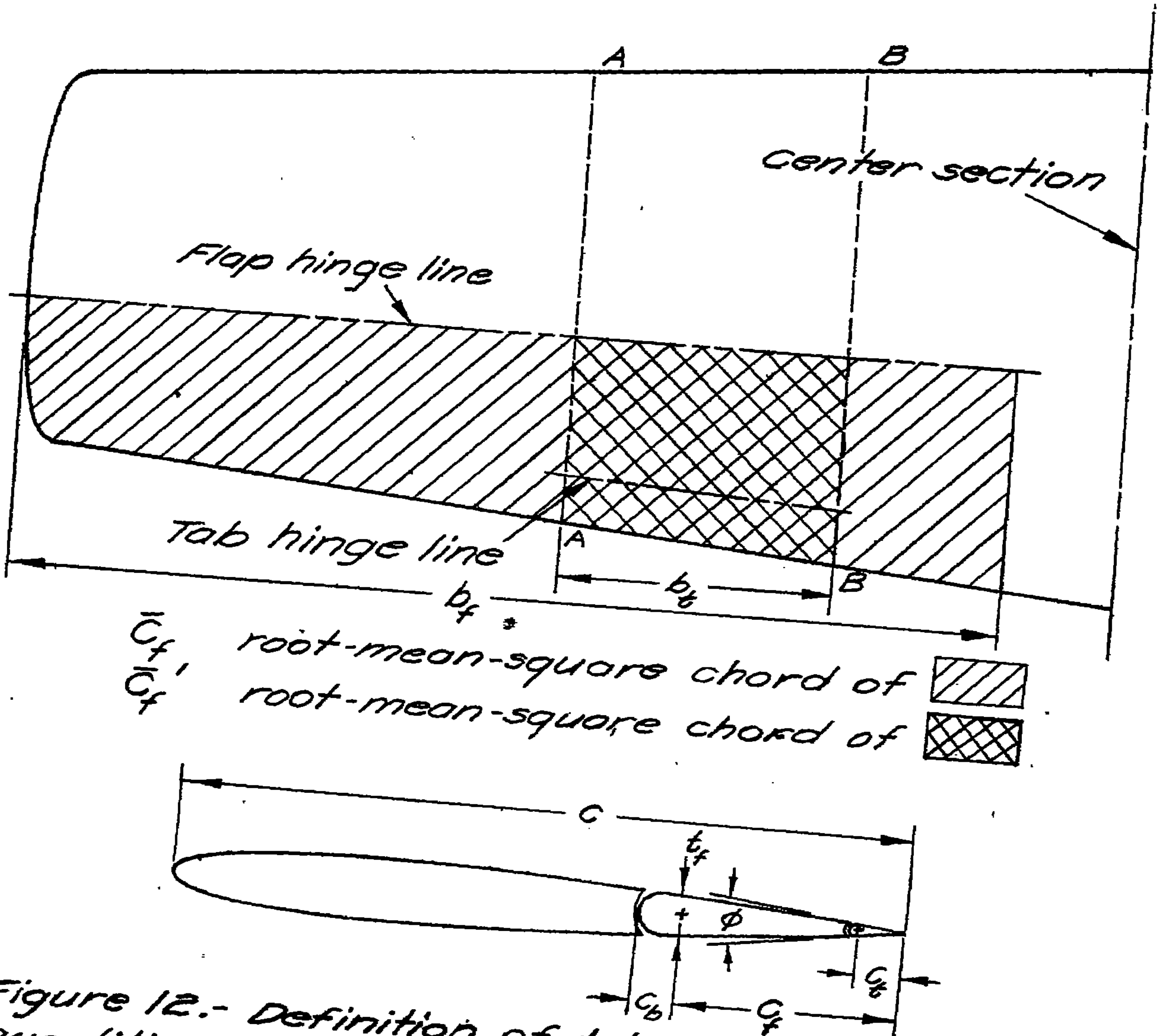

Figure 12.- Definition of tab parameters. The quantities c, t_f, c_b, c_f, c_t, and ϕ are average values for the airfoil sections between section AA and section BB. For thin attached tabs, use for ϕ the trailing-edge angle of the airfoil.

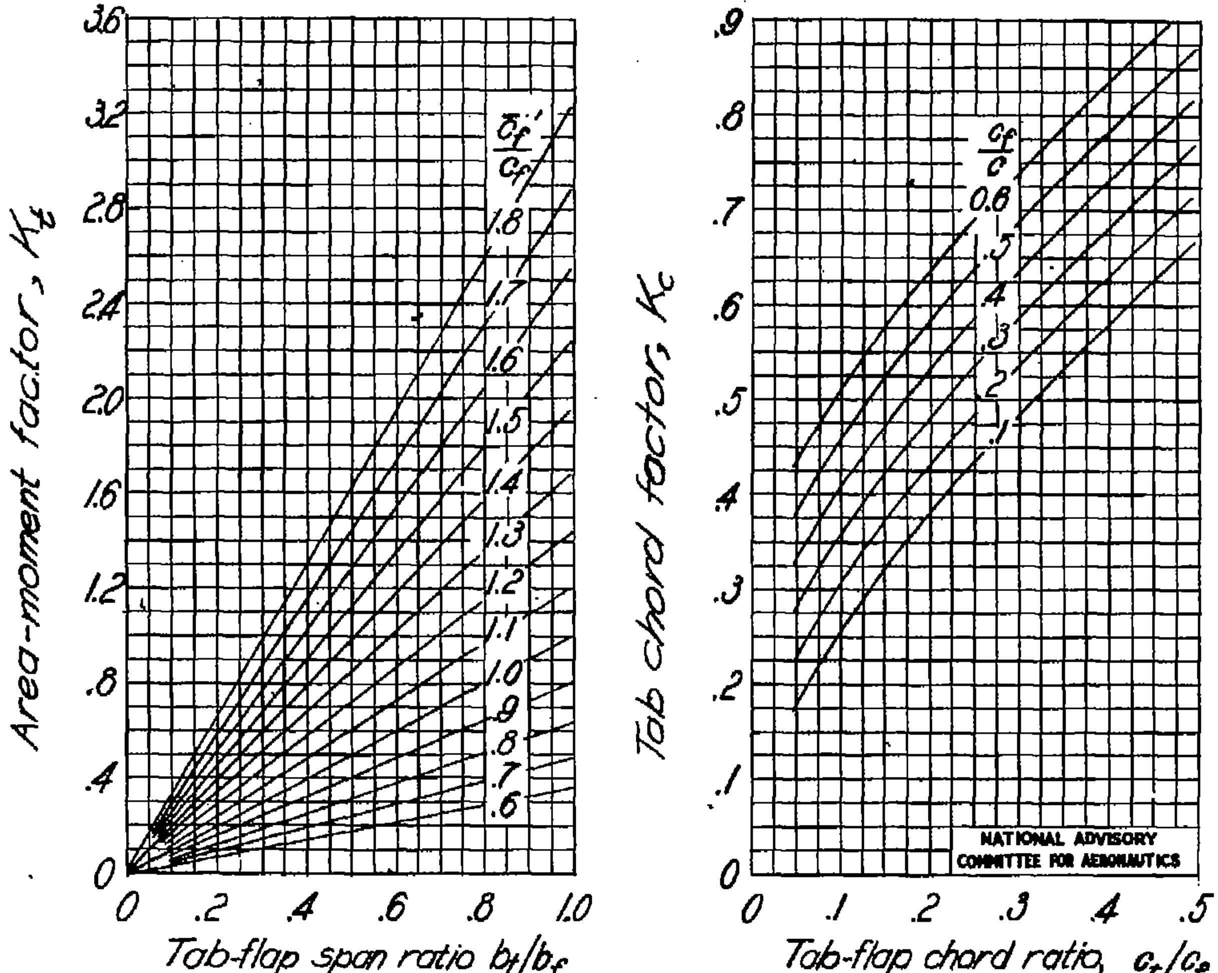

(a) Area-moment factor. (b) Tab chord factor.

Figure 13.- Charts from which tab correlation factors can be determined.

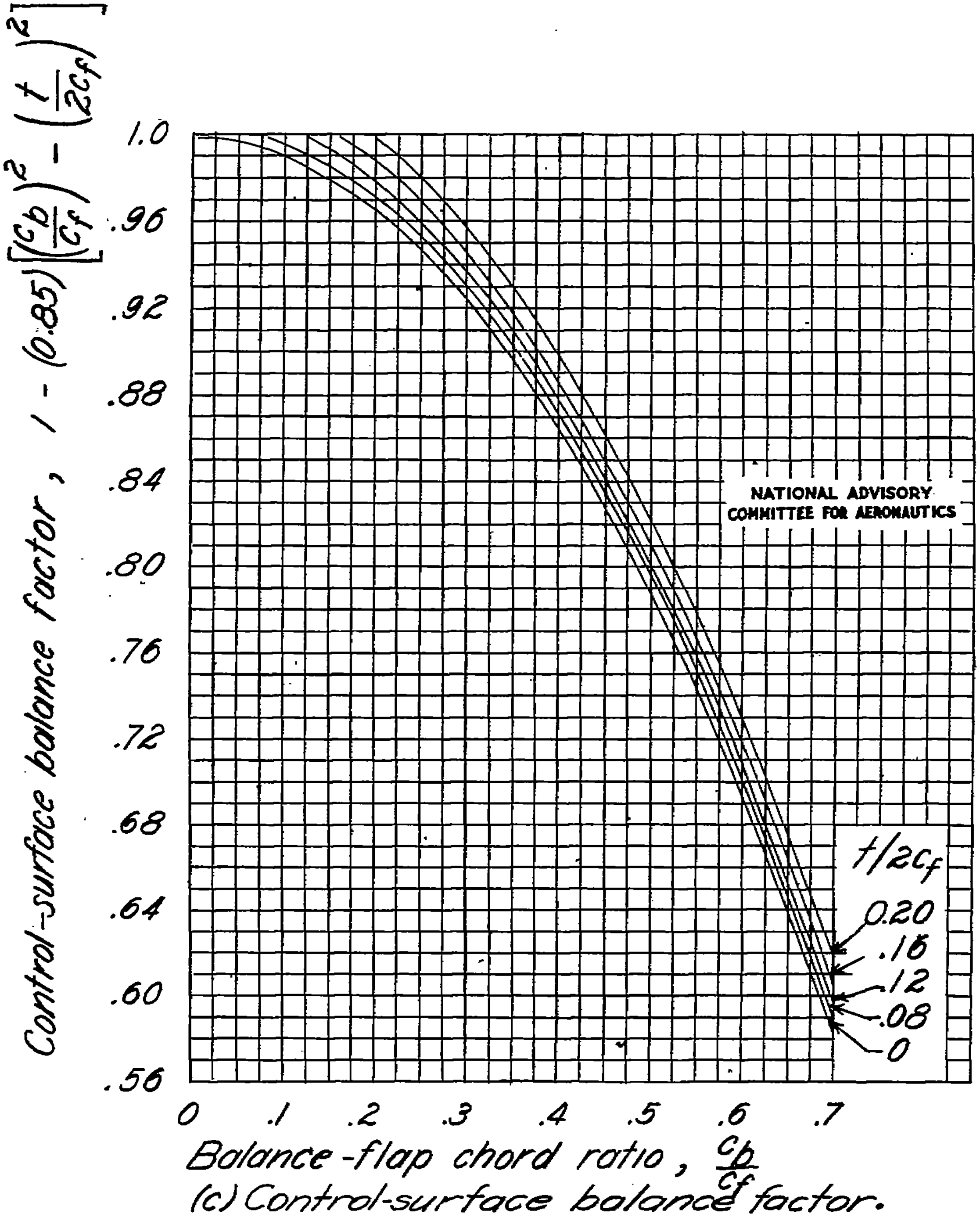

(c) Control-surface balance factor.

Figure 13.-Concluded.